NASA CR-179512

NASA

UNSTALLED FLUTTER STABILITY PREDICTIONS AND COMPARISIONS TO TEST DATA FOR A COMPOSITE PROP-FAN MODEL

J. E. Turnberg

HAMILTON STANDARD DIVISION
UNITED TECHNOLOGIES CORPORATION

October, 1986

Prepared For

NATIONAL AERONAUTICS AND SPACE ADMINISTRATION

Lewis Research Center
Cleveland, Ohio 44135

Contact NAS3-24088

NASA CR-179512

NASA

UNSTALLED FLUTTER STABILITY PREDICTIONS AND COMPARISIONS TO TEST DATA FOR A COMPOSITE PROP-FAN MODEL

J. E. Turnberg

HAMILTON STANDARD DIVISION
UNITED TECHNOLOGIES CORPORATION

October, 1986

Prepared For

NATIONAL AERONAUTICS AND SPACE ADMINISTRATION

Lewis Research Center
Cleveland, Ohio 44135

Contact NAS3-24088

1. Report No.	2. Government Accession No.	3. Recipient's Catalog No.
CR-179512		

4. Title and Subtitle	5. Report Date
Unstalled Flutter Stability Predictions and Comparisons to Test Data for a Composite Prop-Fan Model	October 15, 1986
	6. Performing Organization Code

7. Author(s)	8. Performing Organization Report No.
J. E. Turnberg	HSER 11056
	10. Work Unit No.

9. Performing Organization Name and Address	11. Contract or Grant No.
Hamilton Standard Div., United Technologies Corp. Windsor Locks, CT 06095	NAS3-24088
	13. Type of Report and Period Covered
12. Sponsoring Agency Name and Address	Contractor
National Aeronautics and Space Administration Lewis Research Center 21000 Brookpark Road Cleveland, OH 44135	14. Sponsoring Agency Code

15. Supplementary Notes

Final Report. Technical Monitor - Mr. Oral Mehmed, NASA - Lewis Research Center, Cleveland, Ohio 44135

16. Abstract

This report presents the aeroelastic stability analyses for three graphite/epoxy composite Prop-Fan designs and post-test stability analysis for one of the designs, the SR-3C-X2. The study showed that Prop-Fan stability can be effectively analyzed using the F203 modal aeroelastic stability analysis developed at Hamilton Standard and that first mode torsion-bending coupling has a direct effect on blade stability. Positive first mode torsion-bending coupling is a destabilizing factor and the minimization of this parameter will increase Prop-Fan stability. The study also showed that Prop-Fan stability analysis using F203 is sensitive to the blade modal data used as input. Calculated blade modal properties varied significantly with the structural analysis used, and these variations are reflected in the F203 calculations.

17. Key Words (Suggested by Author(s))	18. Distribution Statement
Flutter, Prop-Fan, Blades, Propeller, Aeroelastic	Unclassified, Unlimited

19. Security Classif. (of this report)	20. Security Classif. (of this page)	21. No. of pages	22. Price*
Unclassified	Unclassified	50	

*For sale by the National Technical Information Service, Springfield, Virginia 22161

FOREWORD

The analytical and experimental work described in this report was conducted through the joint effort of the NASA-Lewis Research Center and the Hamilton Standard Divison of the United Technologies Corporation under NASA contract NAS3-24088. Mr. Oral Mehmed of the NASA Lewis Research Center was the Technical Monitor for the contract.

All of the testing was performed in the NASA-Lewis 8x6 wind tunnel under the direction of Mr. Mehmed. NASA-Lewis personnel provided the structural finite element analytical model and modal data for aeroelastic stability predictions and the test data for comparison with analytical predictions. At Hamilton Standard, Mr. Jay E. Turnberg and Ms. Karen S. Morrell conducted the analytical predictions. Mr. Bennett M. Brooks was the Hamilton Standard Project Manager.

TABLE OF CONTENTS

1.0 SUMMARY

This report presents the aeroelastic stability analyses performed for three graphite/epoxy composite Prop-Fan designs and the post-test aeroelastic stability analysis for one of the designs, the SR-3C-X2. The major objective of this work was to assist NASA-Lewis in the development of two advanced composite Prop-Fan models, one that would be stable to high flight Mach numbers and one that would be unstable at low flight Mach numbers. The stable model, the SR-3C-3, was used for subsequent wind tunnel structural response and stability verification testing. The unstable model, the SR-3C-X2, was subjected to wind tunnel tests in order to obtain flutter data.

This aeroelastic stability study showed that Prop-Fan stability can be effectively analyzed using the F203 modal aeroelastic stability analysis developed at Hamilton Standard and that first mode torsion bending coupling has a direct effect on blade stability. Control of this coupling by composite ply-layer tailoring was the procedure used to produce the stable SR-3C-3 and the unstable SR-3C-X2 models.

The study also revealed that the prediction of Prop-Fan stability using the F203 aeroelastic analysis is sensitive to the blade modal data used as input. Although finite element analysis methods were used to calculate all of the blade modal data for this study, differences in the detailed finite element analysis solution procedures caused variations in the blade modal data that are reflected in the F203 stability predictions.

2.0 INTRODUCTION

The emergence of the Prop-Fan as a fuel conservative competitor to the high bypass ratio turbofan has created new interest in propeller technology development. Both analytical studies and wind tunnel tests at Mach numbers between 0.7 and 0.8 have shown that aerodynamic performance efficiencies of about 80 percent are achievable for single-rotation Prop-Fans (SRP) and efficiencies as high as about 89 percent are achievable for Counter-Rotating Prop-Fans (CRP) (Reference 1).

These high efficiencies have been accompanied by increasing structural demands over those of conventional turbopropellers. Prop-Fans have six or more swept, thin, low aspect ratio blades. These blade characteristics increase the potential for an aeroelastically unstable configuration. This potential was confirmed during testing of a highly swept titanium model Prop-Fan called SR-5 at the NASA Lewis Research Center in the spring of 1981 (Reference 2). The SR-5 model Prop-Fan exhibited an unstalled flutter instability at high Mach number.

The consequence of the SR-5 instability was a re-examination of the unstalled flutter prediction methodology and the development of new unstalled flutter calculation procedures specifically tailored to meet the needs of the Prop-Fan (References 2, 3, 4, and 5). To further investigate flutter in advanced turboprops and to verify analytical procedures, test data in addition to the SR-5 model Prop-Fan test data was required. This need for additional data prompted the development and testing of the SR-3C-X2 model Prop-Fan.

The SR-3C-X2 is a graphite fiber/epoxy matrix composite model Prop-Fan fabricated at the NASA Ames Research Center. It was designed to flutter at a subsonic Mach number and was tested in the NASA Lewis 8x6 wind tunnel. The aerodynamic performance of this model had been previously established from a solid titanium version of the configuration known as the SR-3 (Reference 6). Unstalled flutter has never been observed during wind tunnel tests of the SR-3. In addition to the SR-3C-X2 flutter model, another graphite/epoxy model was developed, designated the SR-3C-3, for stable dynamic response testing. This model, as with the metal SR-3, did not exhibit flutter.

This report is a summary of the flutter blade design selection process, and post-test stability analysis and correlation with data. The program has involved a joint effort between NASA-Lewis and Hamilton Standard personnel. Hamilton Standard provided test and data reduction support for the program in addition to aeroelastic stability analysis for the model. NASA-Lewis provided finite element analysis results for the aeroelastic stability analysis and all hardware and test facilities, conducted the test, and supplied both raw and reduced data.

This work was sponsored by the NASA Advanced Turboprop Project office as part of the overall program to develop advanced turboprop technology.

3.0 DISCUSSION

3.1 Flutter Model Selection

One goal of this program was the development of two composite model Prop-Fans with the geometry of an existing solid titanium model called SR-3. Figure 1 shows the geometric characteristics of the SR-3 Prop-Fan. One of the composite models, the SR-3C-X2, was designed to flutter at a low flight Mach number while the other, the SR-3C-3, was designed to be stable to a high Mach number so that it could be tested for dynamic response on an isolated nacelle (Reference 7).

From previous internal work performed at NASA-Lewis and Hamilton Standard it was determined that Prop-Fan flutter could be controlled by altering the vibratory mode shapes of the blades. Two techniques are generally suitable to alter blade mode shape. One involves changes in the blade external geometry, as was performed to obtain a stable design for the LAP SR-7 Prop-Fan (Reference 8), and the other involves changes in the internal shape or material composition of the blade. Tailoring the composite material ply orientation will alter the structural characteristics but not change the external geometry and was the method selected by NASA-Lewis to create the SR-3C models. An additional factor which must be included in the analysis with either geometric or composite tailoring is the effect of the blade retention and hub flexibilities. For this study the retention and hub could be considered rigid so the flexibilites were not included in the analysis. In general full scale designs have bearing retentions and flexible hubs that must be included in the mode shape and frequency calculations for subsequent stability predictions.

The type of flutter examined for this study is a predominant first mode flutter. This type of flutter is greatly influenced by blade sweep, torsion-bending coupling in the first in vacuo mode, and the aerodynamic coupling of the first in vacuo mode to higher in vacuo modes (Reference 5). A distinction is made here between in vacuo modes and aerodynamically coupled modes. A flutter mode is an aerodynamically coupled mode. Unsteady aerodynamic loads introduce stiffness and damping into the structure which modify the frequencies and mode shapes of the in vacuo structure and alter blade stability. Therefore a Prop-Fan operating in a wind tunnel or under flight conditions has mode shapes and frequencies that are altered with each change in rotational speed, wind tunnel or flight speed, and air density or altitude. The extent to which the air interacts with the Prop-Fan is related to the mass, stiffness and geometric properties of the Prop-Fan.

Blade sweep introduces a destabilizing unsteady aerodynamic force component into the system when the first in vacuo mode shape of the blade has zero or positive torsion-bending coupling. Torsion-bending coupling is defined by:

$$\lambda = \frac{\theta b}{h} \qquad (1)$$

where torsion (θ) is defined as rotation of an airfoil cross section about the line tangent to the geometric mid-chord sweep curve shown in Figure 1. A positive sign is given for leading edge-up rotation. Bending (h) is defined as the translation of the mid-chord in the direction normal to the blade surface with a positive sign convention for translation toward the airfoil face (pressure) side, as illustrated in Figure 2, and blade dimension (b) is the semi-chord.

The natural tendency of an aft swept blade is to vibrate in the first mode with positive torsion-bending coupling because of the overhung tip mass introduced by sweep. This natural tendency to vibrate in the first mode with positive torsion-bending coupling can be altered by tailoring the composite ply orientation. Therefore, to select high and low stability composite SR-3 models, NASA-Lewis personnel examined a number of composite ply configurations of which three were selected as candidates for flutter analysis, the SR-2C-X2, SR-3C-3, and the SR-3C-X7. These three configurations differed only in ply orientation. Of these configurations, the SR-3C-X2 and the SR-3C-3 were built, so that the structural analyses could be verified.

The material composition of these models is a layered build-up of graphite prepreg unidirectional tape with each layer, or ply, oriented in the following specified directions. Figure 3 shows the nominal graphite ply fiber orientation for the three configurations that were analyzed for flutter during the model selection process. The SR-3C-X2 had a (-22.5°, 0°, 22.5°) ply lay-up that made the model flexible in torsion and brought the first and second mode natural frequencies close together. The SR-3C-3 had a (-45°, 0°, 45°) ply lay-up to provide increased torsional rigidity. The third configuration, the SR-3C-X7, had a (-45°, 0°, 7.5°, 45°, 52.5°) ply orientation that increased the frequency separation between modes 1 and 2, and uncoupled the bending and torsional motion in the first mode. All three configurations were constructed with the same type of epoxy matrix and graphite ply material so the mass distribution remained nearly constant. The effect of the stiffness variation due to ply orientation is shown by examination of the blade natural frequencies in Table I and the blade mode shapes in Figures 4, 5, and 6.

A comparison of the displacement contours for the first mode in Figures 4, 5, and 6 shows contours with decreasing slope for the SR-3C-X2, SR-3C-3, and SR-3C-X7 models, respectively. The slope of these displacement contour lines is indicative of the magnitude of the torsion-bending coupling. A summary of the torsion-bending coupling for the first mode is shown in Figure 7. At the blade tip, where the greatest aerodynamic forces are encountered, the SR-3C-X2 model is shown to have the greatest amount of torsion-bending coupling and, therefore, should have the lowest stability of the three configurations.

The predicted first mode damping for the three proposed composite SR-3 model Prop-Fans, shown in Figure 8, indicated that the assumed low stability of the SR-3C-X2 is supported by analysis. The stability prediction, was performed for the three Prop-Fan configurations rotating at 8636 RPM with sea level aerodynamic conditions. The critical flutter velocities for the SR-3C-X2, SR-3C-3 and the SR-3C-X7 are Mach 0.28, Mach 0.68 and greater than Mach 1.0, respectively. A review of the stability predictions showed that two Prop-Fan models, the SR-3C-X2, and the SR-3C-3, would satisfy the requirements of this program and future programs. That is to have both high and low stability composite Prop-Fan models, with the geometric shape of the SR-3.

Although the SR-3C-3 model shows a critical flutter velocity of Mach 0.68, it was selected to be the high stability model because Mach 0.68 represents the critical flutter velocity at sea level conditions. This is a lower critical flutter velocity than would be anticipated during testing, since the model is run in a wind tunnel with an equivalent altitude of approximately 6000 ft at Mach 0.8. The decreased dynamic pressure in the wind tunnel increases stability. Another reason why the SR-3C-3 was selected over the SR-3C-X7 was because it had the potential, according to calculations, to flutter at a Mach number outside the operating range of the planned response test based on extrapolation of calculated sea level stability to wind tunnel test condition so that flutter data could be obtained in addition to high speed response data. Further information regarding the high stability model, the SR-3C-3, is found in Reference 7. The SR-3C-3 did not flutter during testing. The stability analysis used for this study is described in detail in Reference 3, and will be described in general in Section 3.3. The remainder of the report will deal only with the low stability model, the SR-3C-X2.

3.2 Experiment Description

The SR-3C-X2 model Prop-Fan was tested by NASA-Lewis personnel in the NASA-Lewis 8x6-foot wind tunnel during October of 1983. The 0.61 m (2.04 ft) diameter model was mounted on an isolated nacelle test rig with the thrust axis aligned with the freestream flow. The experiment was conducted at freestream velocities from 0.36 to 0.75 Mach number, with rotor speeds up to 8000 RPM. The blades were mounted in a hub which can be considered to be rigid. Signals from blade mounted strain gages were recorded on FM analog magnetic tape, and also were monitored during the test to identify the

stability boundary of the model. The model was tested in two rotor configurations, first with eight blades and second with four blades to investigate aerodynamic coupling effects between the blades at flutter. Flutter occurred over a wide range of operating conditions for both operating configurations. A detailed description of the experiment and the results can be found in Reference 9. The only data that will be presented here are those that will be used for comparison to the analysis.

The SR-3C-X2 model fluttered in the first aerodynamically coupled mode when operating over a wide range of Mach number and rotational speed in both the eight and four bladed configurations. During flutter all blades vibrated at the same frequency but at different amplitudes and with a common predominate phase angle between adjacent blades. The eight-bladed configuration fluttered with either a 180° or 225° interblade phase angle or with both angles simultaneously. While the four-bladed configuration fluttered with a 180° interblade phase angle (Reference 9).

The measured blade natural frequencies from spectral analysis of wind tunnel strain data are given in the Campbell plot shown in Figure 9, along with the COSMIC NASTRAN predicted blade natural frequencies. There are substantial discrepancies between the rotating measured and predicted frequencies for the modes. The first mode frequency is greater than that predicted while the second mode is lower than that predicted. The frequencies of the third and fourth modes could not be ascertained from the test data with any degree of accuracy. Comparison of non-rotating calculations and static shake tests for the SR-3C-X2, Table II, do not show the frequency discrepancies. The frequency calculations are well within the range of the shake test data. Note that the measured values show large blade-to-blade differences for all the modes, indicating that the assembled model was somewhat mis-tuned from a blade frequency standpoint.

A portion if not all of the frequency discrepancy between the rotating measured and calculated first and second mode frequencies is due to aerodynamic effects. The calculations were performed "in vacuo", without including the influence of aerodynamics. The measured wind tunnel data show a substantial aerodynamic effect. The effect of aerodynamic forces on the blade natural frequency will be addressed further when the stability predictions are discussed.

3.3 Analytical Predictions and Comparisons to Test

The analytical stability predictions for the SR-3C-X2 model were performed using the F203 aeroelastic stability analysis. Briefly, the F203 aeroelastic stability analysis is a modal analysis that was specifically tailored to model the structural and aerodynamic complexities of the Prop-Fan. The complicated geometry of the Prop-Fan is modeled using the torsion-bending coupling shown in Figure 7. The unsteady 2D aerodynamics for the analysis are modeled to account for sweep, compressibility, cascade effects, and

blade tip losses. The solution for the equations of motion takes the form of a complex eigenvalue problem that yields frequency, damping, and complex mode shapes for the system.

The analysis procedure took the following overall approach. First, Hamilton Standard recommended to NASA for analysis three test conditions where flutter occurred. NASA-Lewis approved the test conditions and five cases were developed by NASA-Lewis for finite element analysis to assess the prediction methodology. These five cases plus the pre-test case are summarized in Table III. NASA-Lewis supplied Hamilton Standard with finite element modal data for the analysis cases and stability predictions were made by Hamilton Standard using the modal data assuming two model rotor configurations, eight blades and four blades, to investigate aerodynamic coupling between the blades.

Three different finite element procedures were applied to the blade to assess the effect of finite element procedure on stability predictions. The three techniques are as follows: COSMIC NASTRAN without steady aerodynamic loads (cases 1 and 2), MSC NASTRAN without steady aerodynamic loads (case 3), and finally MSC NASTRAN with steady aerodynamic loads (cases 4, 5, and 6) as summarized in Table III. Cases 2, 3, and 4 form a consistent set of runs for evaluating the sensitivity of stability to the finite element analysis procedure for a single test operating condition.

The comparison between the two NASTRAN programs, COSMIC and MSC, was performed to assess how differences in solution procedures and element formulations alter the blade stability results. MSC NASTRAN was also run using two procedures; one that accounted for steady aerodynamic loads and the other did not account for the steady aerodynamic loads. The effect of steady aerodynamic loads is to deflect the blade into a new mean position, and as noted previously, the blade mode shapes are directly related to the mean position of the blade.

The choice of finite element procedure did yield substantial variations in the modal data for cases 2, 3, and 4. These variations are summarized by frequencies in Table IV and mode shapes in Figure 10. For the three comparison cases (2, 3 and 4) the predicted first mode frequency varies over a range of only 6.0%, but the amount of first mode torsion-bending coupling varies from 0.09 to 0.36 at the 80% radial station. Variations of this magnitude directly affected the subsequent stability predictions.

The MSC NASTRAN with airloads finite element procedure used on cases 4, 5, and 6 is the most sophisticated. The calculations include steady aerodynamic loads and geometric nonlinearities. It was initially thought that this procedure would best represent the blade structurally, but even this solution technique shows an inconsistency. The predicted natural frequencies of modes 2 and 3 do not increase with rotational speed. Case 6 at 6400 RPM shows a second mode frequency of 400 Hz, while case 5 at 7368 RPM shows a decreased second mode frequency of 364 Hz. The MSC NASTRAN with airloads analysis indicates that the frequency decreases with

increasing rotational speed, which is an unlikely phenomenon for the primary modes of a Prop-Fan blade. This also is not supported by test data for this blade or by the pre-test COSMIC NASTRAN frequency predictions shown in Figure 9.

The stability predictions made using these modal data were performed for an eight-bladed configuration and a four-bladed configuration. It should be noted that the four-bladed SR-3C-X2 stability calculations, made using MSC NASTRAN with airloads finite element calculations, contain steady airloads developed for the eight-bladed configuration. Therefore, these four-blade stability predictions contain a known approximation, eight-bladed steady airloads. All stability predictions were performed using the first six normal modes to represent the blades in the calculations.

Eight Bladed Comparisons - The six cases were analyzed in an eight-bladed configuration for point-to-point comparison to test results. Predicted first mode damping and frequency plots for these cases are shown in Figures 11 through 16. The first mode is predicted to go unstable for each case at the predicted point of zero damping. The flutter Mach numbers and frequencies for this configuration are listed in Table V and displayed in Figure 17.

In all cases the upper bound Mach number for blade stability was under-predicted. The correlation between prediction and test data varied for each case. To begin the discussion of the comparison between prediction and test data, the results from the three modal calculation procedures, case 2, case 3, and case 4, representing the 6100 RPM, Mach 0.6 test run 879 will be examined.

The three calculations for this flutter point show a variation in flutter Mach number from 0.45 to 0.55. The COSMIC NASTRAN, case 2, results showed the lowest upper bound Mach number for blade stability with a flutter Mach number of 0.45. This is an under-prediction, of the tested flutter Mach numer of 0.60, by 25%. The change to MSC NASTRAN, case 3, increased the predicted stability to Mach 0.55, which is an 8% under-prediction. Finally, the addition of steady aerodynamic loads to the MSC NASTRAN modal calculations lowered the previous prediction to Mach 0.54, which is a 10% under-prediction. The results show that predictions using MSC NASTRAN modal data gave better correlation to test results than the COSMIC NASTRAN modal data for this flutter point. Also, the inclusion of steady aerodynamic loads in the modal data calculation procedure produced a small change in predicted stability. The overall under-prediction of stability may, in part, be due to the exclusion of any structural damping in the calculations. Structural damping increases blade stability.

A comparison of the point-to-point predictions using MSC NASTRAN with airloads, cases 4, 5, and 6, to the test values shows that the case 6 at 6400 RPM result produced the best correlation with test data. The calculation is within 3% of the tested upper bound Mach number for blade stability for run 985. As discussed previously, the case 4 prediction at 6100 RPM is within 10% of the tested run 879 stability. Case 5 at 7368 RPM does not correlate well with the

test data, and the calculation is inconsistent with the other predictions. Case 5 under-predicts the onset of blade instability, for run 904, by 82%.

The inconsistencies in the stability predictions follow the differences found in the modal data. Comparing the finite element study cases 2, 3, and 4, representing run 879, case 2 had far more torsion-bending coupling than cases 3 and 4, and therefore was predicted to be less stable. For the point-to-point comparison cases, the cause of deviation for case 5 is not clear, although it was noted previously that the frequency predictions show a low value for the second mode. This is not in agreement with any of the other analytical results, or the test data. This indicates that some problems specific to this modal calculation may exist.

Since the results from case 5 were out of agreement with the other predictions, further investigation into the difference was performed. A comparison was made between two test operating conditions with tip helical Mach numbers of about 0.85. These two conditions were case 5 at Mach 0.5 and 7386 RPM and case 6 at Mach 0.6 and 6400 RPM.

Constant tip helical Mach number was selected as a basis for the comparison because this establishes similar aerodynamic velocity distributions. Even though the aerodynamic conditions are similar for these calculations, the stability predictions are grossly different. Case 6 shows a first mode viscous damping ratio and frequency prediction of -0.015 and 283 Hz, while case 5 shows a first mode viscous damping ratio and frequency prediction of -0.11 and 287 Hz. More insight into the difference can be obtained when the eigenvectors for the two conditions are examined, see Table VI. Case 6 shows 15% coupling between modes one and two while case 5 shows 28% coupling between modes one and two. This increased coupling is destabilizing and is due to modal differences arising from the finite element results.

For the eight-bladed stability predictions, cascade effects were important because of the close blade spacing. When blades are closely spaced, the motion of an adjacent blade affects the stability of the blade under investigation, therefore, the Prop-Fan was analyzed as a system of eight identical blades. The eight blades were allowed to vibrate in eight possible system modes with the following inter-blade phase angles 0°, 45°, 90°, 135°, 180°, 225°, and 315°. The predicted least stable inter-blade phase angle was generally 135°, as shown in Figure 18. The predicted angle differs from the measured phase angle by sign. The measured inter-blade phase angle was 225° or 180° which is equivalent to minus 135° or 180 . The reason for the phase polarity difference between the analysis and experiment is not presently understood and warrants further investigation. The disagreement in inter-blade phase angle between test and calculation had no effect on establishing the stability boundary, because damping at the least stable inter-blade phase angle was used for all of the eight-bladed calculations.

Four-Bladed Comparisons - The six cases were also analyzed for the four-bladed configuration to assess blade interaction effects. The predicted damping and frequency for the first four modes are shown in Figures 19 through 24. The figures show predicted first mode instability to occur at the wind tunnel Mach numbers summarized in Table VII. A review of the predicted eight and four-bladed flutter Mach numbers in Tables V and VII show that the four-bladed configuration is predicted to be stable at higher Mach numbers than the eight-bladed configuration, which is in agreement with the test results. Unfortunately, the variations in predicted stability due to the variations in predicted modal data, discussed previously with the eight-bladed configuration, are also transferred to the four-bladed stability predictions.

The predictions listed in Table VII are compared to test results in Figure 25. From this Figure it is clear that cases 3, 4, and 6 are in good agreement with the test results, while cases 1 and 2 show low predicted stability, and finally, case 5 is out of agreement with all the other predictions, as well as the test results as occurred with eight blades.

Earlier, it was mentioned that the in vacuo frequency predictions did not correlate well with wind tunnel test results, and that part of the discrepancy was due to steady state aerodynamic effects. The effect that unsteady aerodynamic forces have on the blade frequency is shown in Table VII. Aerodynamic forces tend to raise the predicted first mode frequency by approximately 60 Hz at the flutter conditions. This represents a 30% increase in the first mode frequency, which brings it in agreement with the measured values. A review of Table IV and Figures 19 through 24 shows that the second mode frequency is lowered by approximately 30 Hz due to aerodynamic effects. This is also in the direction of better agreement with the test results shown in Figure 9. It is evident, for this blade, that unsteady aerodynamic forces significantly alter the natural frequencies of the blades.

4.0 CONCLUSIONS AND RECOMMENDATIONS

Based on the F203 analytical prediction results and comparisons to experimental data for the SR-3C-X2 and SR-3C-3 model Prop-Fans, the following conclusions and recommendations are made concerning Prop-Fan unstalled flutter analysis.

1) The F203 modal aeroelastic stability analysis was effective as a design tool in developing the SR-3C-X2 and the SR-3C-3 Prop-Fan models.

2) Pre-test F203 stability predictions for the SR-3C-X2 and SR-3C-3 were confirmed when the SR-3C-X2 fluttered and the SR-3C-3 did not flutter.

3) Positive first mode torsion-bending coupling is a destabilizing factor on Prop-Fan unstalled flutter stability and the minimization of this parameter will increase Prop-Fan stability.

4) The SR-3C-X2 eight-bladed configuration was predicted to be less stable than the four-bladed configuration in agreement with test data.

5) Both test data and F203 calculations show that unsteady aerodynamic loads alter the SR-3C-X2 blade in vacuo natural frequencies at rotating conditions.

6) Calculated blade modal properties varied significantly with the structural analysis used, and these variations are reflected in the F203 calculations.

7) The modal characteristics of the SR-3C-X2 need to be re-examined both analytically and experimentally to better assess the F203 aeroelastic stability analysis.

8) A polarity difference found between the predicted and measured least stable inter-blade phase angles warrants further investigation.

5.0 REFERENCES

1. Weisbrich, A. L., J. Godston, and E. Bradley "Technology and Benefits of Aircraft Counter Rotation Propellers", NASA CR-168258, December 1982

2. Mehmed, O., K.R.V. Kaza, J. F. Lubomski, and R. E. Kielb, "Bending-Torsion Flutter of a Highly Swept Advanced Turboprop", NASA Technical Memorandum 82975, 1982

3. Turnberg, J. E., "Classical Flutter Stability of Swept Propellers", 83-0847-CP, AIAA/ASME/ASCE/AHS 24th Structures, Structural Dynamics and Materials Conference, May 2-4, 1983

4. Elchuri, V., G.C.C. Smith, "Flutter Analysis of Advanced Turbopropellers", 83-0846-CP, AIAA/ASME/ASCE/AHS 24th Structures, Structural Dynamics and Materials Conference, May 2-4, 1983

5. Bansal, P. N., P. J. Arseneaux, A. F. Smith, J. E. Turnberg, and B. M. Brooks, "Analysis and Test Evaluation of the Dynamic Response of Three Advanced Turboprop Models", NASA CR-174814, August 1985.

6. Rohrbach, C., F. B. Metzger, D. M. Black, and R. M. Ladden, "Evaluation of Wind Tunnel Performance Testings of an Advanced 45° Swept Eight-Bladed Propeller at Mach Numbers from 0.45 to 0.85," NASA CR 3505, March 1982

7. Smith, A. F. and B. M. Brooks "Dynamic Response Test of an Advanced Composite Prop-Fan Model" NASA CR-179528, 1986.

8. Sullivan, William E., Jay E. Turnberg, John A. Violette "Large-Scale Advanced Prop-Fan (LAP) Blade Design", NASA CR 174790, 1985.

9. Mehmed, O. and K.R.V. Kaza, "Classical Flutter Experiment Using a Composite Advanced Turboprop Model", NASA TM 88792, July 1986.

TABLE I

CALCULATED NATURAL FREQUENCIES FOR THE COMPOSITE SR-3C MODEL PROP-FANS*

Frequency ~ Hz (Zero RPM/8636 RPM)

Mode	SR-3C-X2	SR-3C-3	SR-3C-X7
1	189/230	194/242	195/244
2	380/411	448/506	454/484
3	687/704	640/739	717/806
4	744/889	876/963	868/932
5	1074/1073	1122/1183	1138/1151
6	1149/1117	1202/1225	1240/1282

*Furnished by NASA-Lewis

TABLE II

COMPARISON BETWEEN CALCULATED AND MEASURED NATURAL FREQUENCIES FOR THE SR-3C-X2 COMPOSITE MODEL PROP-FAN AT ZERO RPM

	Frequency ~ Hz	
Mode	Calculated	Measured*
1	189	188 - 208
2	380	367 - 387
3	687	666 - 696
4	744	699 - 728

*Range of measured frequencies for all eight blades tested. Measurements and calculations performed by NASA-Lewis.

TABLE III

SUMMARY OF RUNS AND ANALYSIS CASES FOR THE SR-3C-X2 ANALYSIS

Analysis Conditions			Analysis Procedure			
RPM	ß3/4	Mach* No.	Analysis Case	NASTRAN Type	Steady Airloads	No. of Blades
8636	58.0	Pre-Test	1	Cosmic	No	4 8
6100	61.6	0.6	2	Cosmic	No	4 8
			3	MSC	No	4 8
			4	MSC	Yes	4 8
7368	61.6	0.45	5	MSC	Yes	4 8
6400	56.6	0.6	6	MSC	Yes	4 8

*Mach no. only valid with steady airloads.

TABLE IV

PREDICTED BLADE NATURAL FREQUENCIES
FOR THE SR-3C-X2 MODEL PROP-FAN*

In vacuo*/In air** Frequency ~ Hz

Case	FEA Analysis Type	RPM	ß3/4	Mode 1	Mode 2	Mode 3	Mode 4
1	Cosmic	8636	58.0°	230/275**	411/390	704/630	889/880
2	Cosmic	6100	61.6°	220/287	401/385	697/660	816/825
3	MSC	6100	61.6°	212/270	400/365	681/620	822/825
4	MSC/Airloads	6100	61.6°	207/275	387/355	682/620	809/810
5	MSC/Airloads	7368	61.6°	208/260	364/315	655/615	842/820
6	MSC/Airloads	6400	56.6°	212/280	400/370	690/620	820/820

*In vacuo calculations furnished by NASA Lewis.

**In air frequency at the zero damping condition shown in Figures 20 thru 25 calculated by Hamilton Standard using NASA-Lewis in vacuo modal data.

TABLE V

PREDICTED AND MEASURED FLUTTER STABILITY FOR THE SR-3C-X2 IN AN EIGHT-BLADED CONFIGURATION

Case	Conditions		β3/4	Flutter Mach No.		Flutter Frequency Hz	
	Test Run No.	RPM Analysis/Test		Predicted	Measured	Predicted	Measured
1	Pre-test	8636/----	58.0°	0.1	-	270	-
2	879	6100/6070	61.6°	0.45	0.60	280	268
3	879	6100/6070	61.6°	0.55	0.60	260	268
4	879	6100/6070	61.6°	0.54	0.60	260	268
5	904	7368/7400	61.6°	0.08	0.45	245	274
6	986	6400/6385	56.6°	0.58	0.60	280	274

TABLE VI

PREDICTED EIGENVECTORS FOR TWO SR-3C-X2 CONDITIONS

Case 6 Mach 0.6 6400 RPM

135° interblade phase angle

Mode	Eigenvector	Coupling to Mode 1, %
1	0.3391 - 0.9169i	100
2	-0.1170 + 0.1012i	15
3	-0.0594 + 0.0622i	9
4	-0.0210 + 0.0197i	3
5	-0.0065 + 0.0070i	1
6	-0.0002 + 0.0002i	0

Case 5 Mach 0.5 7386 RPM

135° interblade phase angle

Mode	Eigenvector	Coupling to Mode 1, %
1	0.06352 - 0.9980i	100
2	-0.2652 - 0.0883i	28
3	-0.0756 + 0.0655i	10
4	0.0395 - 0.0311i	5
5	0.0149 - 0.0140i	2
6	0.0001 + 0.0001i	0

TABLE VII

PREDICTED AND MEASURED FLUTTER STABILITY FOR THE SR-3C-X2 IN A FOUR-BLADED CONFIGURATION

Case	Analysis Conditions RPM	ß3/4	Predicted Flutter Mach No.	Predicted Flutter Freq.~Hz	Predicted In vacuo Freq.~Hz	Measured Approx. Freq.~ Hz
1	8636	58.0°	0.17	275	230	-
2	6100	61.6°	0.52	287	220	272
3	6100	61.6°	0.64	270	212	272
4	6100	61.6°	0.62	275	207	272
5	7368	61.6°	0.18	260	208	264
6	6400	56.6°	0.65	280	212	276

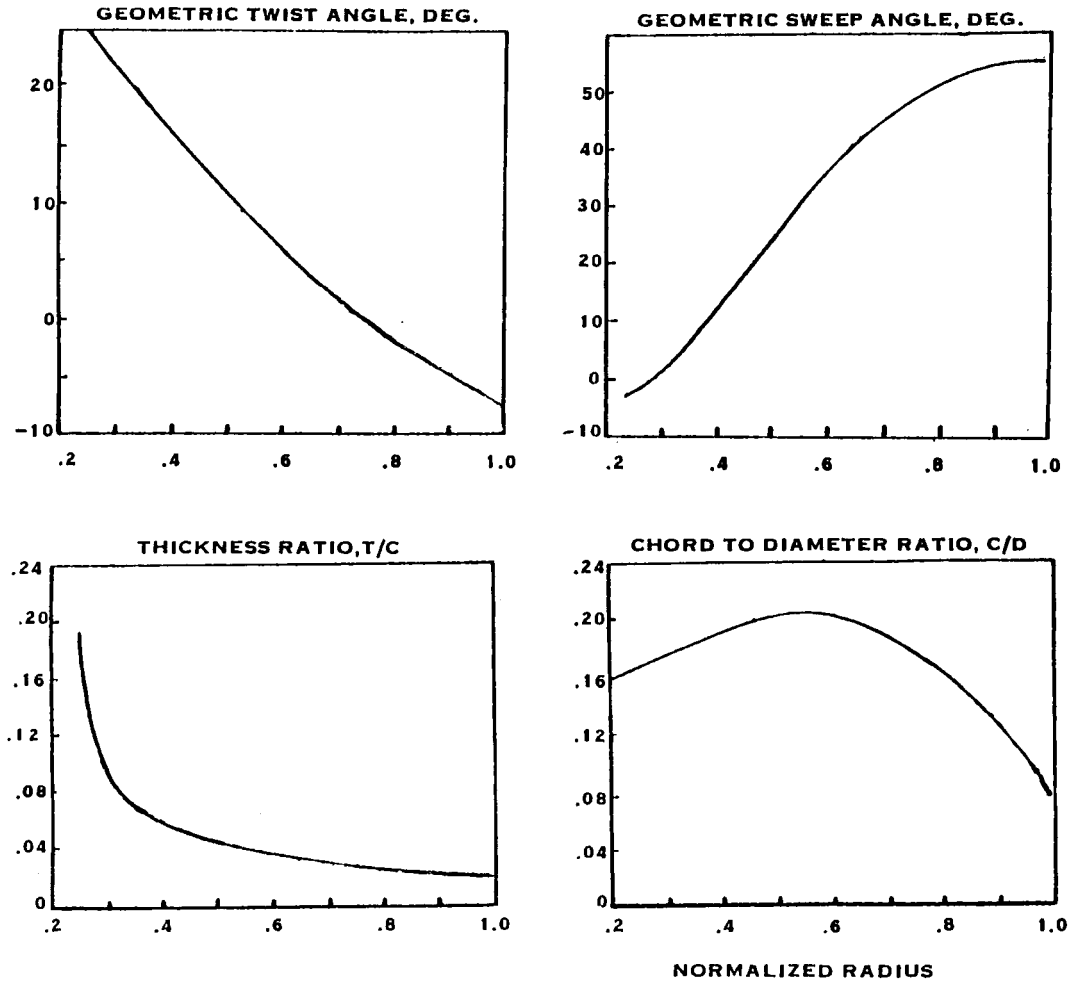

FIGURE 1 SR-3 GEOMETRIC PROPERTIES

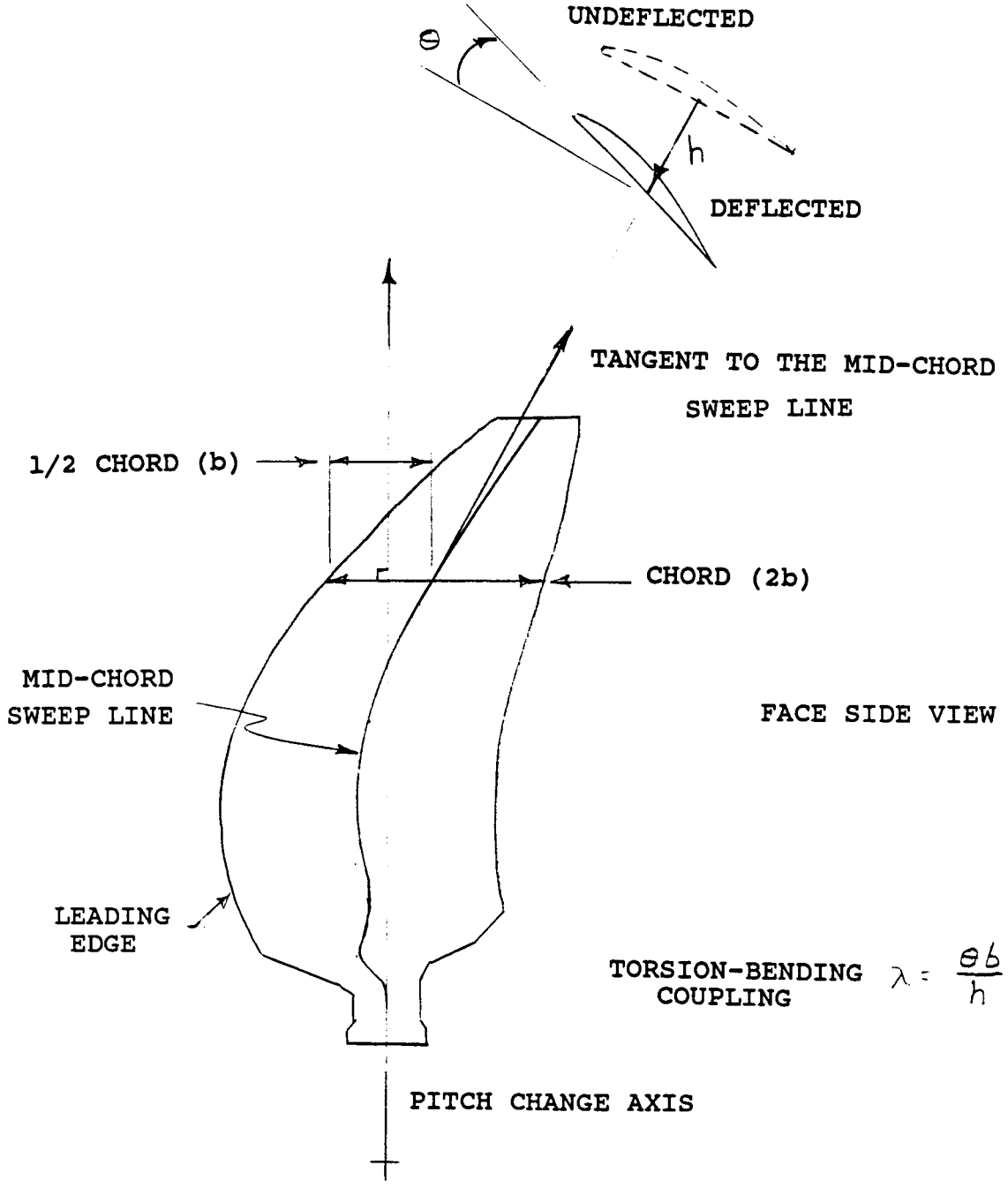

FIGURE 2 DEFINITION OF MODAL DISPLACEMENTS FOR TORSION-BENDING COUPLING

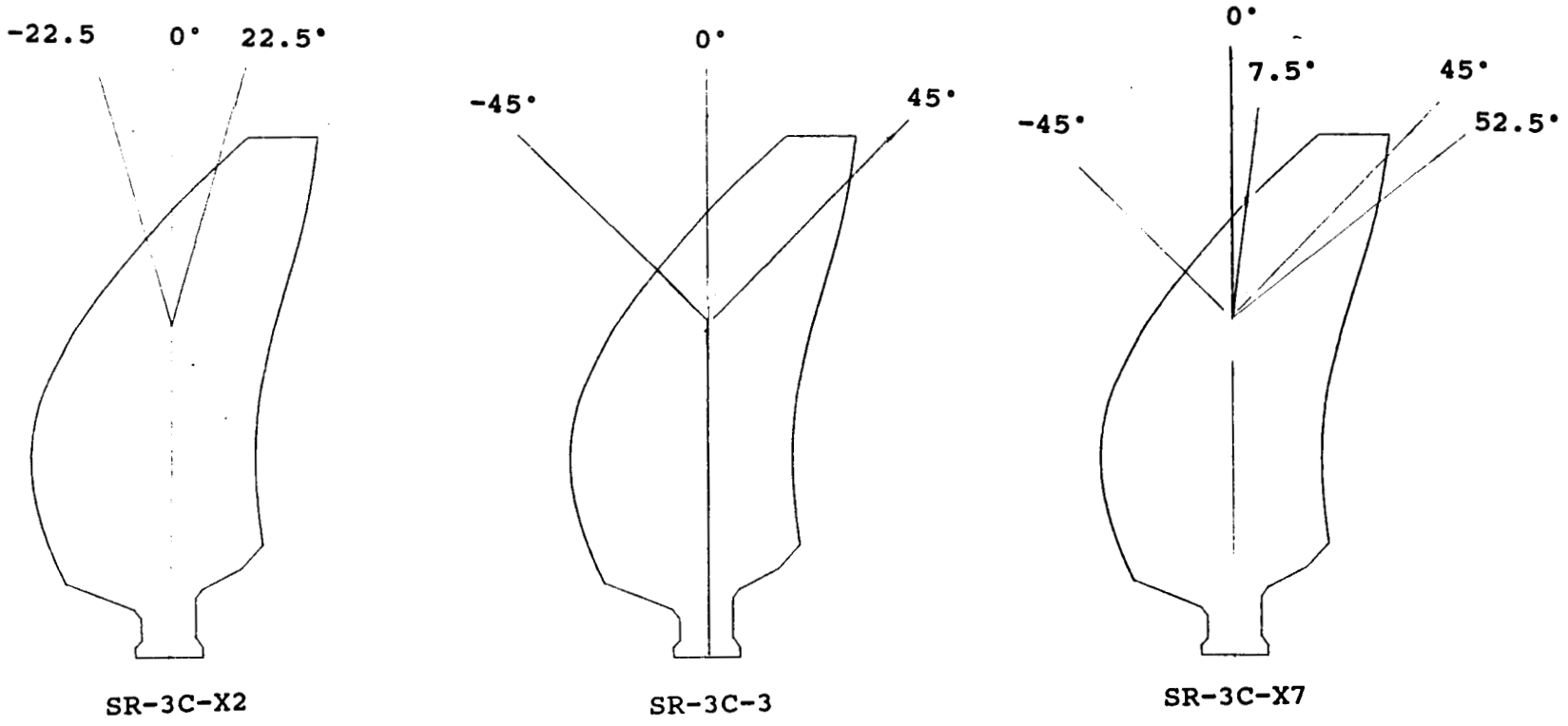

FIGURE 3 GRAPHITE PLY ORIENTATIONS FOR THREE COMPOSITE SR-3 MODEL PROP-FANS

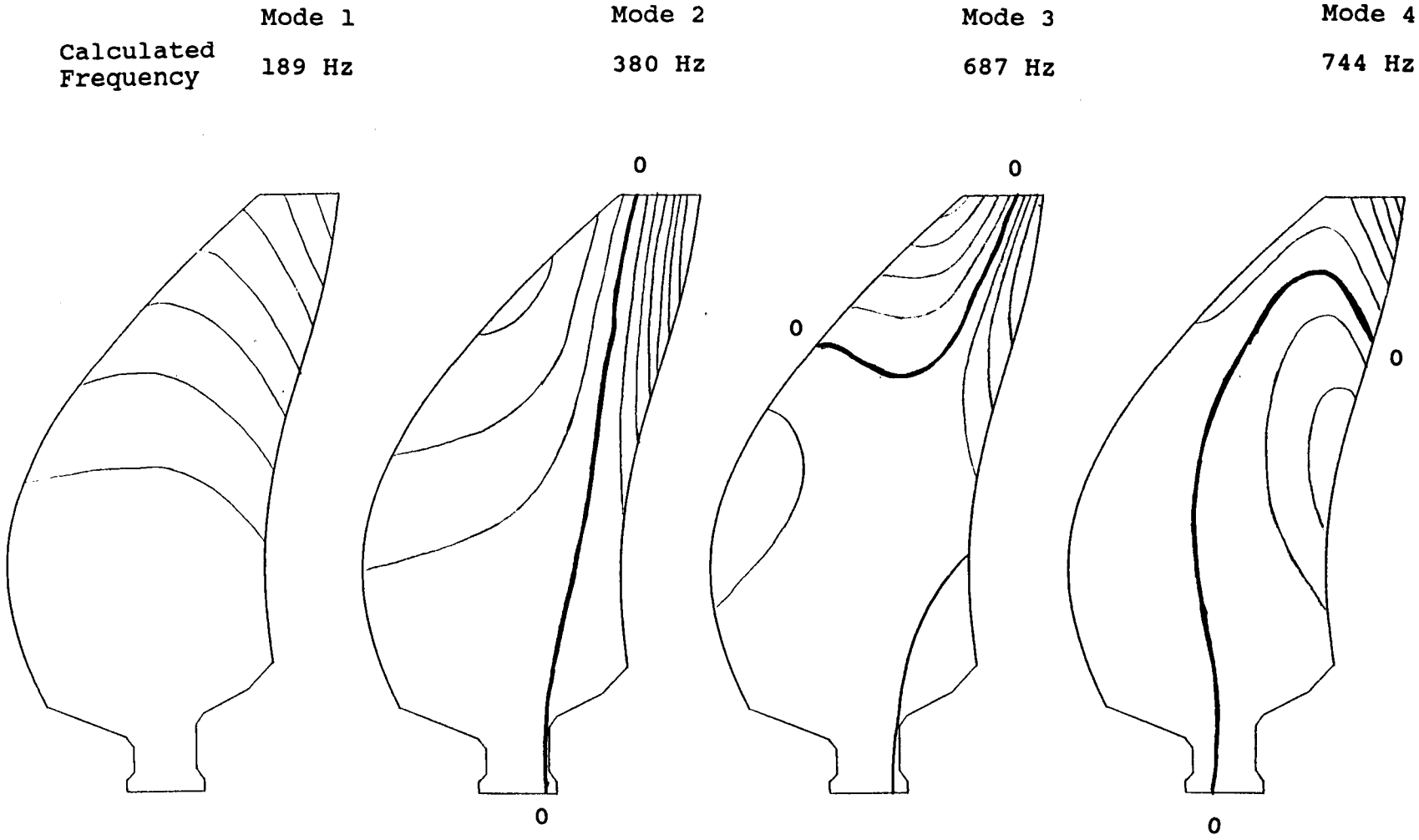

FIGURE 4 NASA-LEWIS SR-3C-X2 COMPOSITE MODEL PROP-FAN MODE SHAPE AND FREQUENCY PREDICTIONS AT ZERO RPM

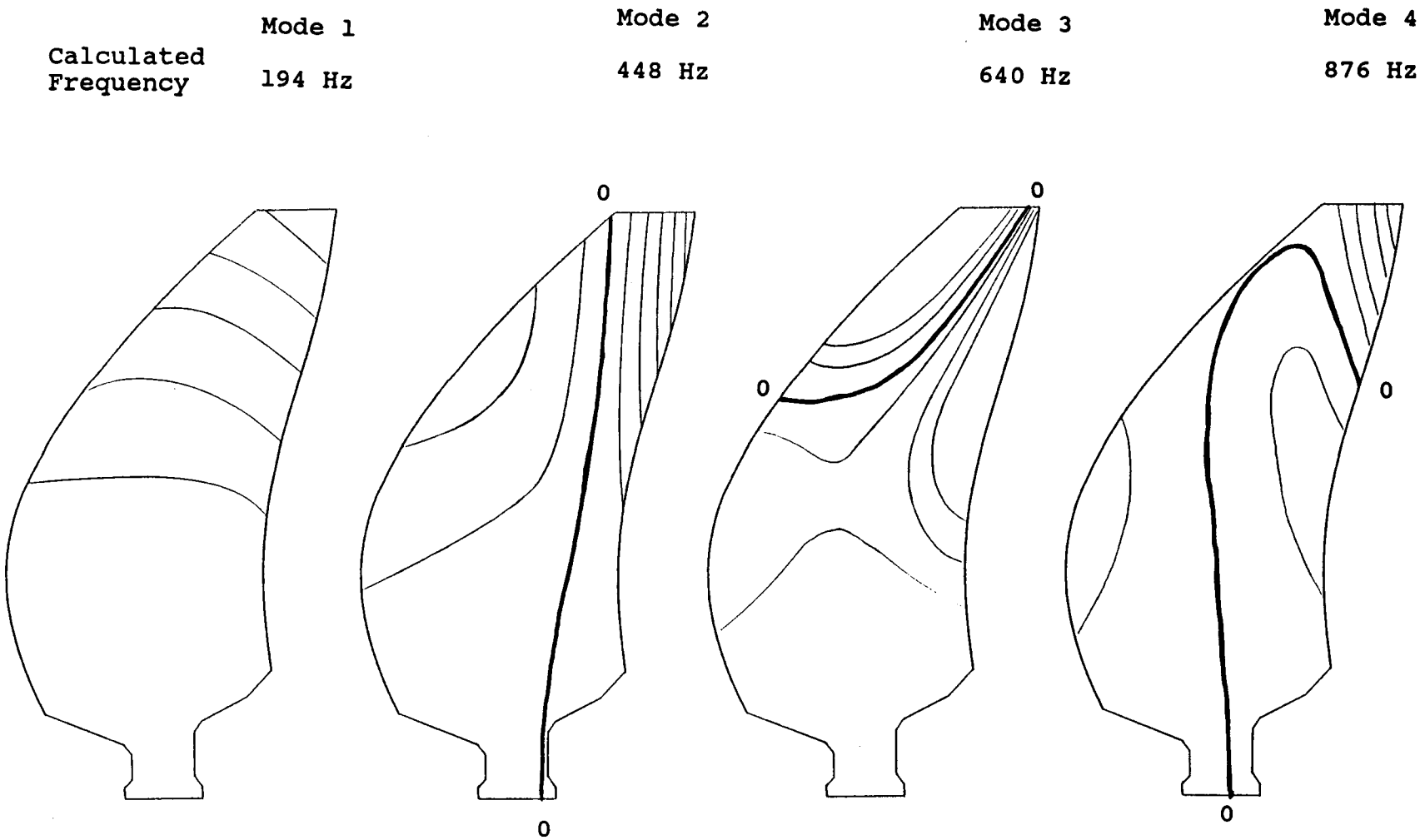

FIGURE 5 NASA-LEWIS SR-3C-3 COMPOSITE MODEL PROP-FAN MODE SHAPE AND FREQUENCY PREDICTIONS AT ZERO RPM

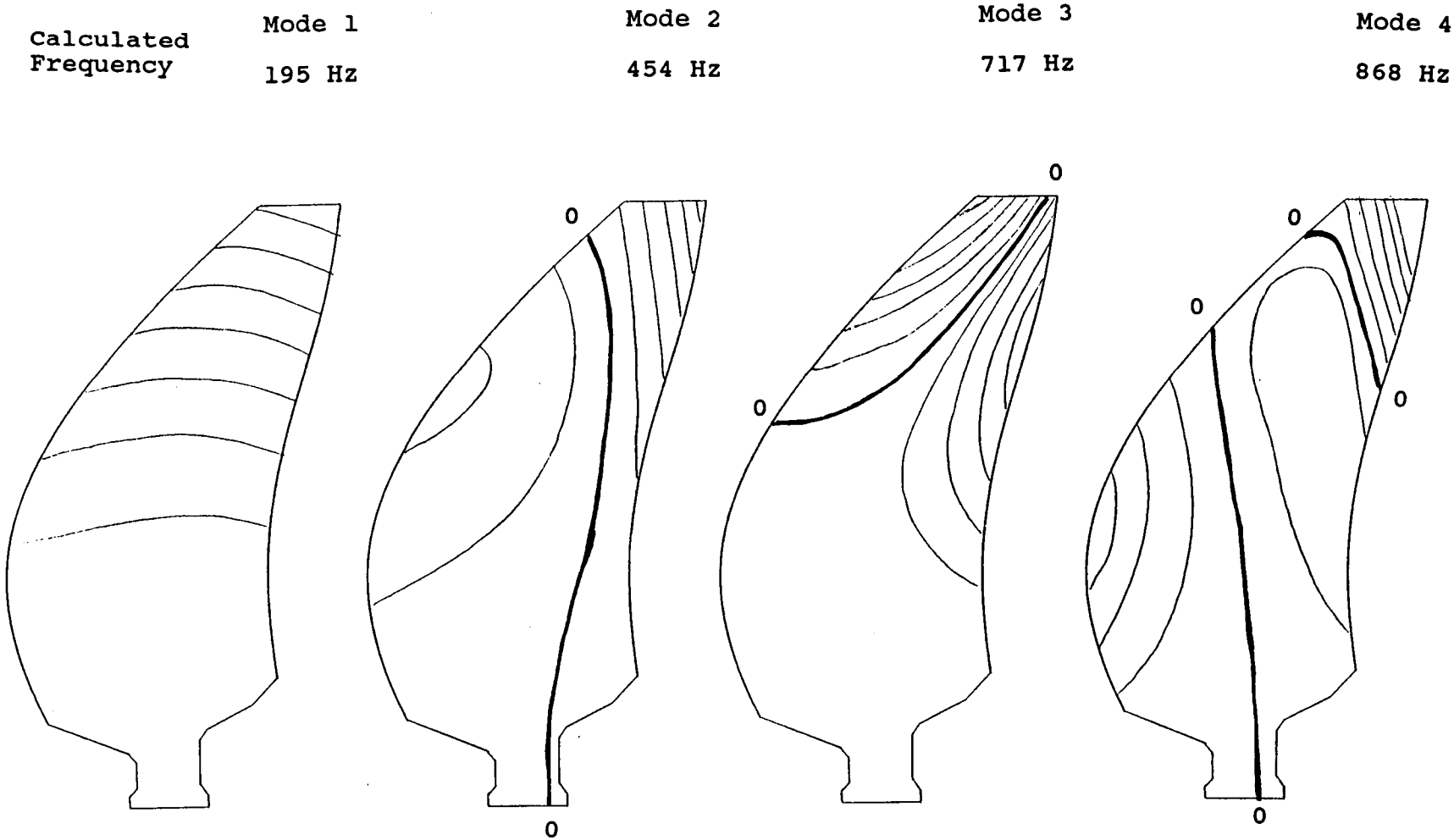

FIGURE 6 NASA-LEWIS SR-3C-X7 COMPOSITE MODEL PROP-FAN MODE SHAPE AND FREQUENCY PREDICTIONS AT ZERO RPM

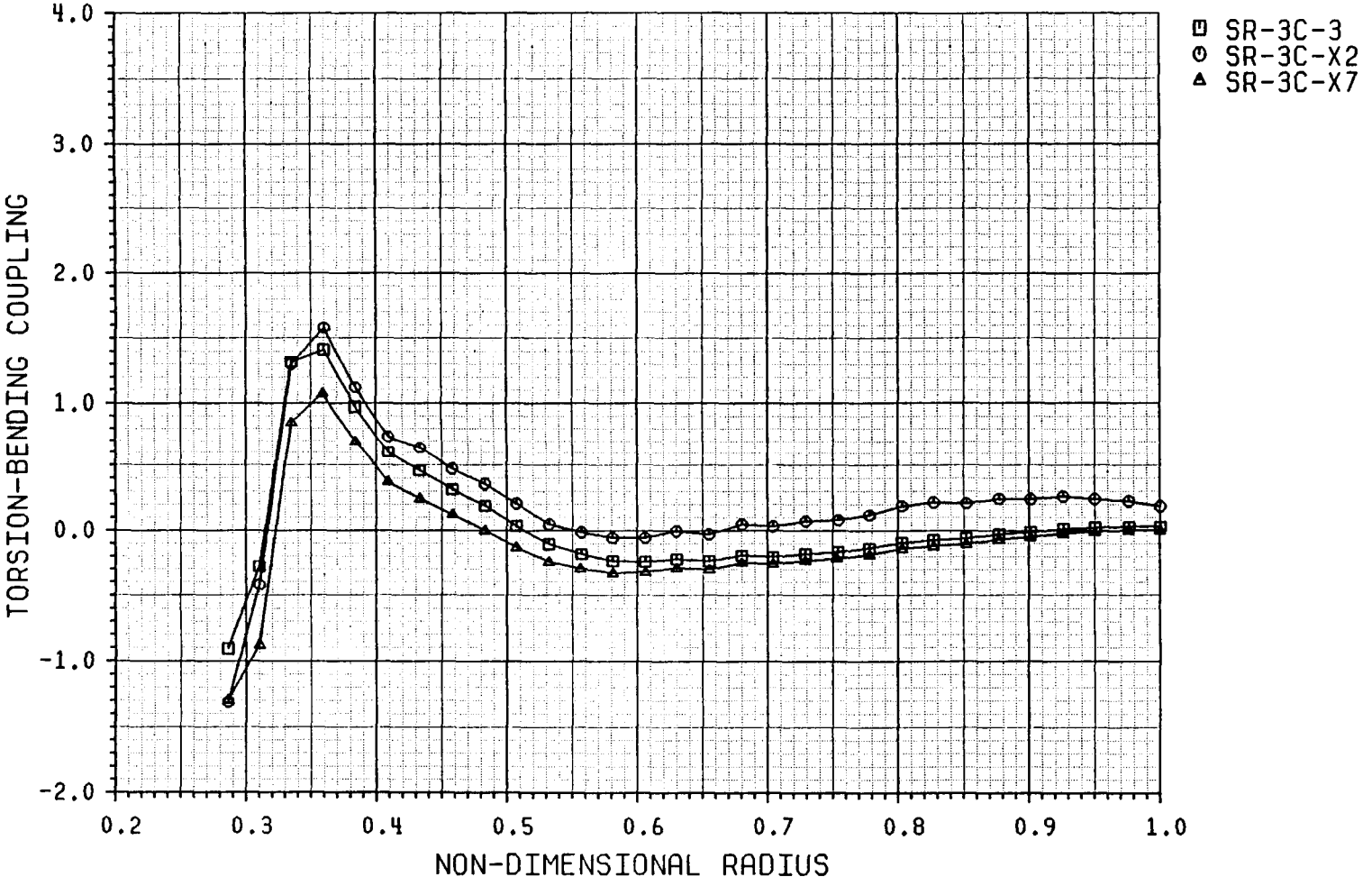

FIGURE 7 FIRST MODE TORSION-BENDING COUPLING FOR THREE PROPOSED COMPOSITE SR-3 MODEL PROP-FANS AT 8636 RPM, $\beta_{3/4} = 58°$ IN VACUO

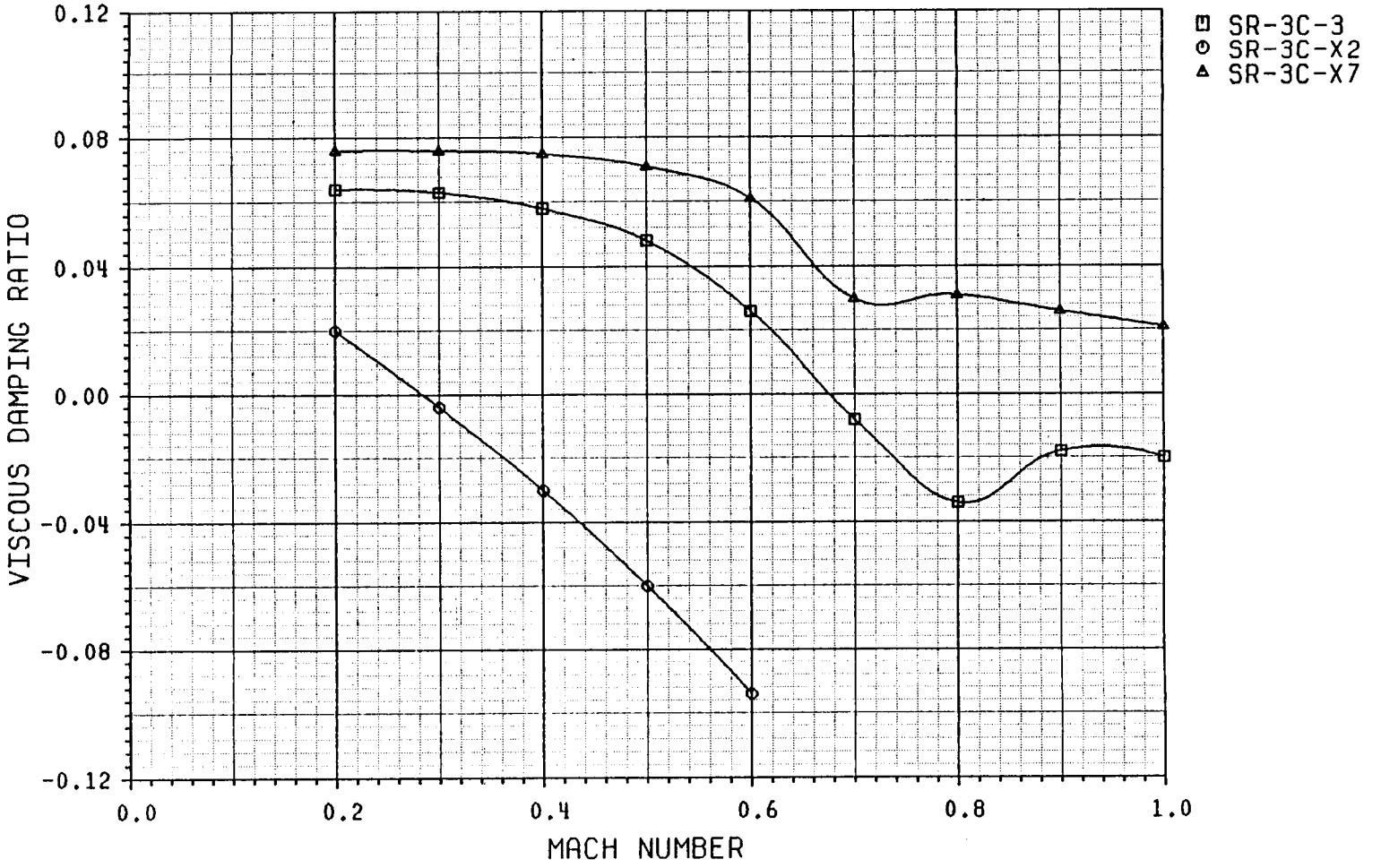

FIGURE 8 PREDICTED FIRST MODE DAMPING FOR THREE PROPOSED COMPOSITE SR-3 MODEL PROP-FANS OPERATING AT 8636 RPM, $\beta_{3/4} = 58°$.

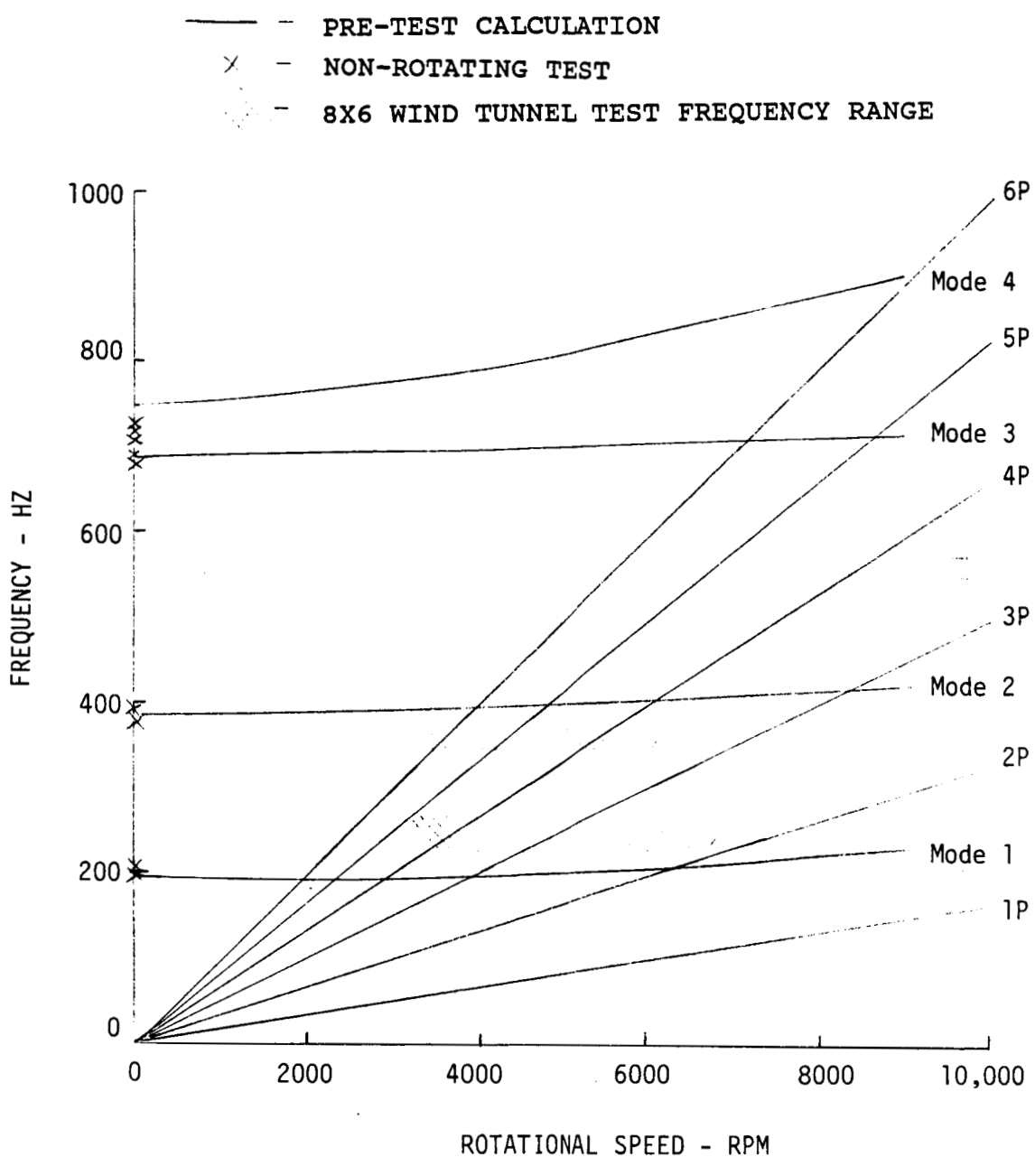

FIGURE 9 COMPARISON BETWEEN PRE-TEST IN VACUO NATURAL FREQUENCY PREDICTIONS WITH MEASURED BLADE NATURAL FREQUENCIES IN AIR

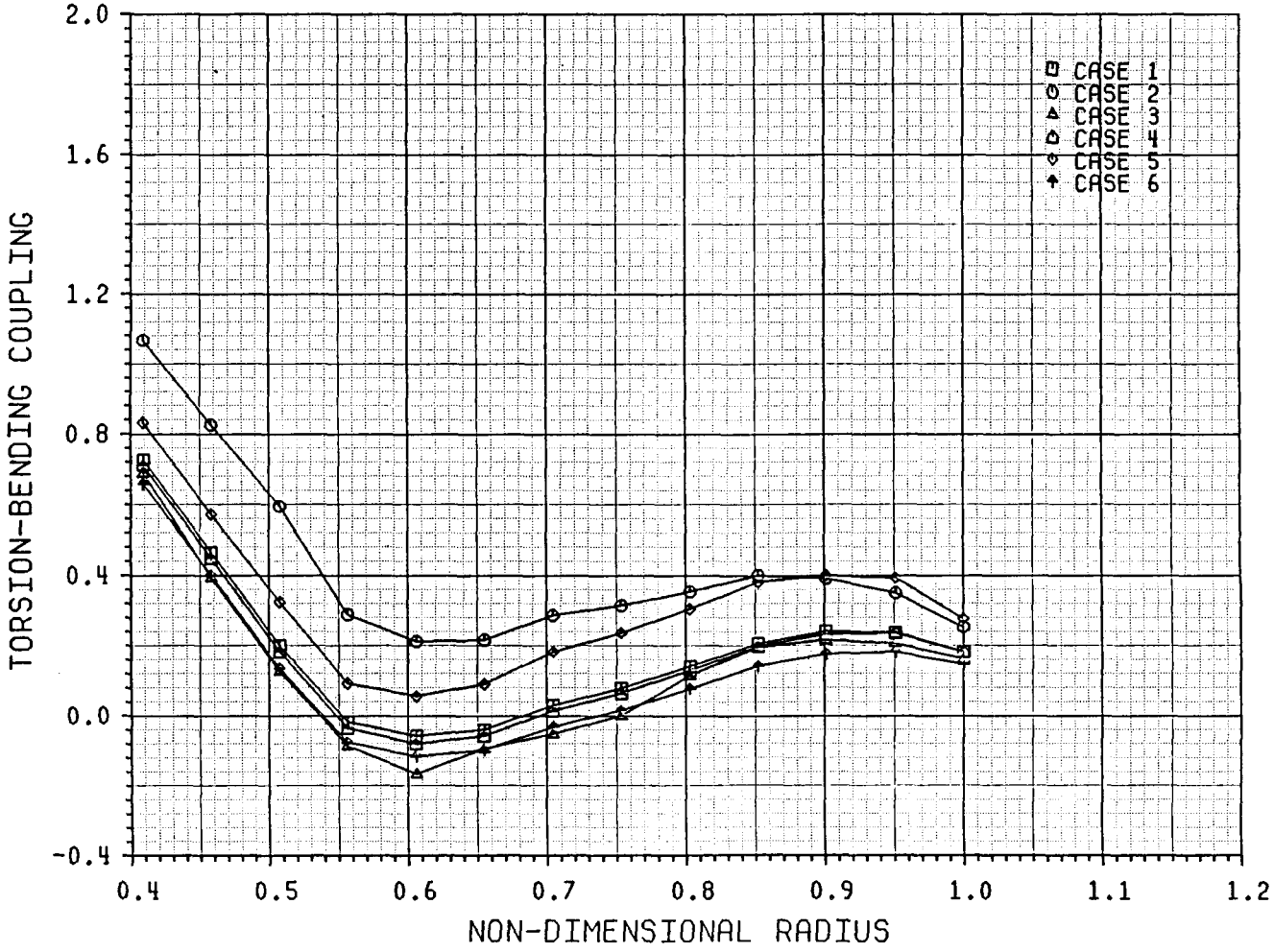

FIGURE 10 FIRST MODE TORSION-BENDING COUPLING FOR THE SIX FINITE ELEMENT ANALYSIS SR-3C-X2 CASES

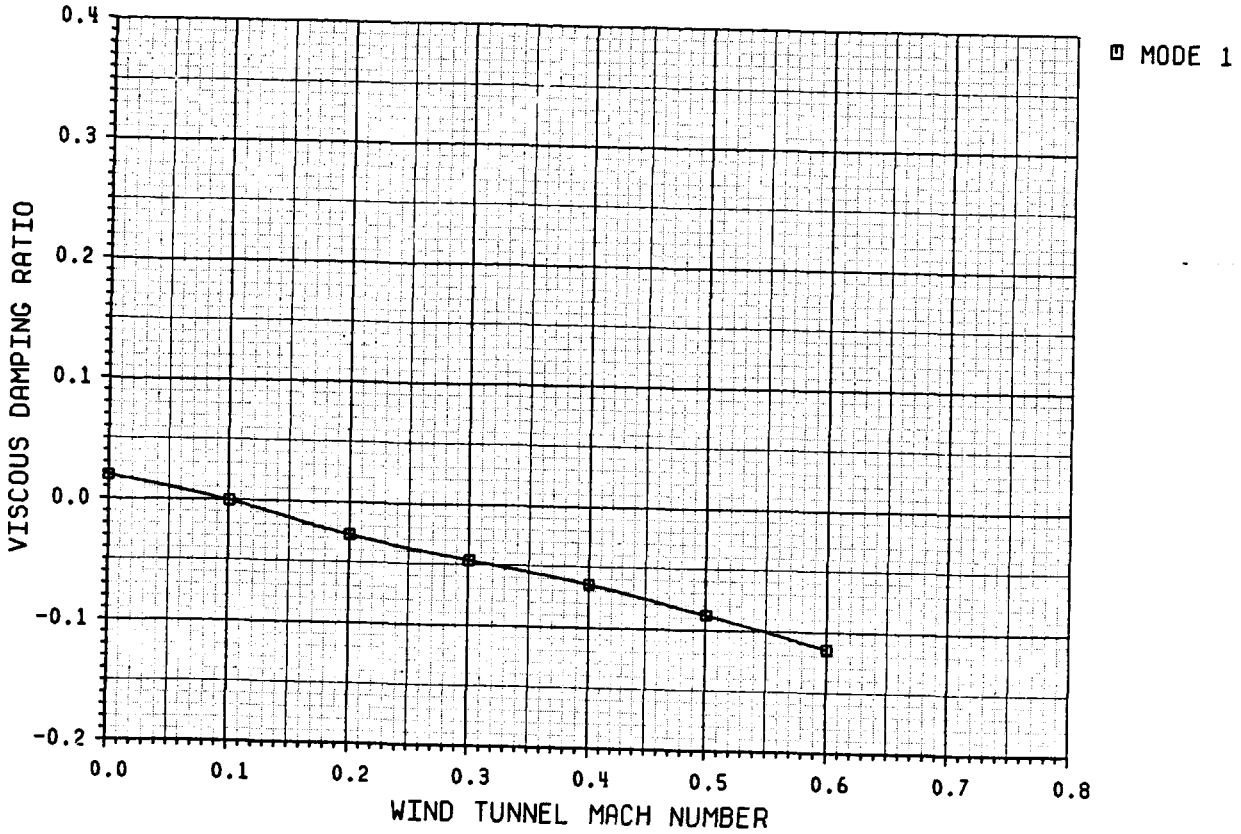

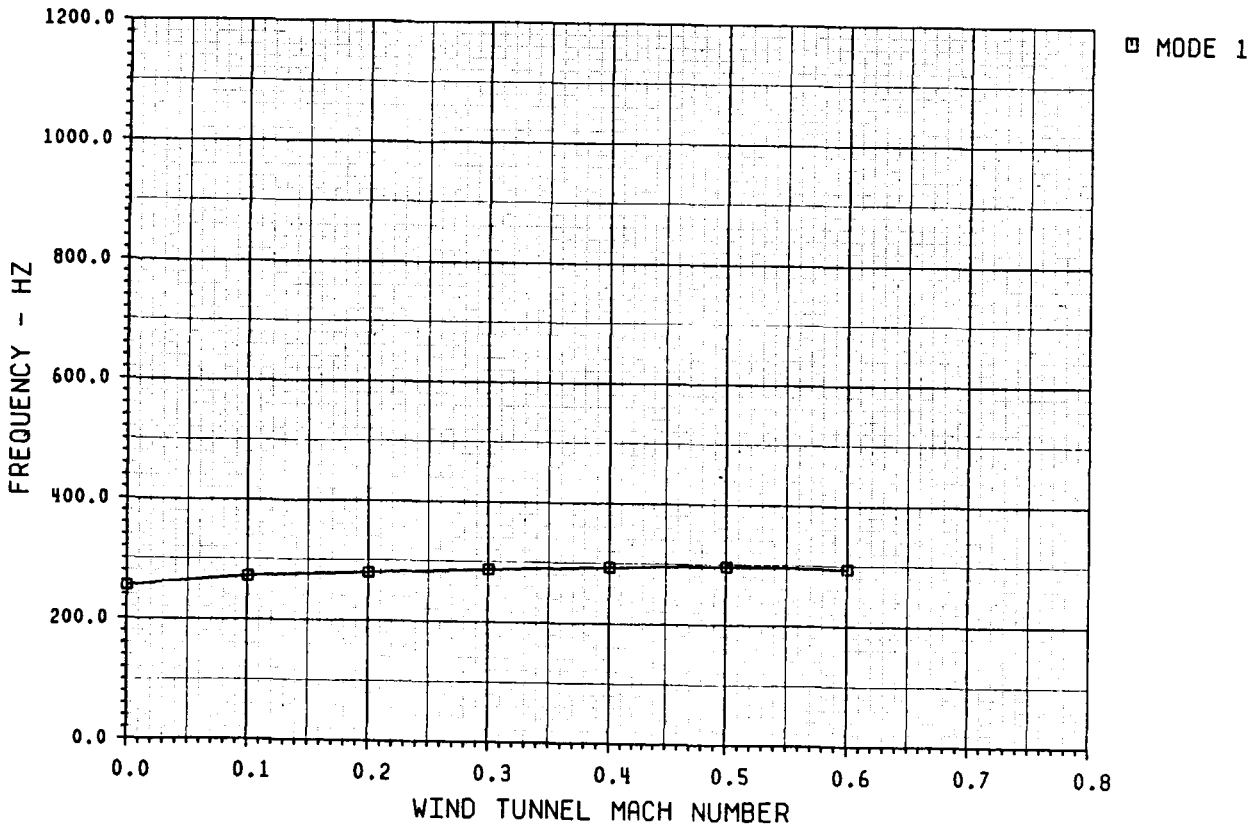

FIGURE 11 SR-3C-X2 STABILITY PREDICTION FOR AN EIGHT-BLADED CONFIGURATION USING CASE 1 MODAL DATA AT 8636 RPM, $\beta_{3/4}$ = 58°, COSMIC NASTRAN, NO STEADY AIRLOADS

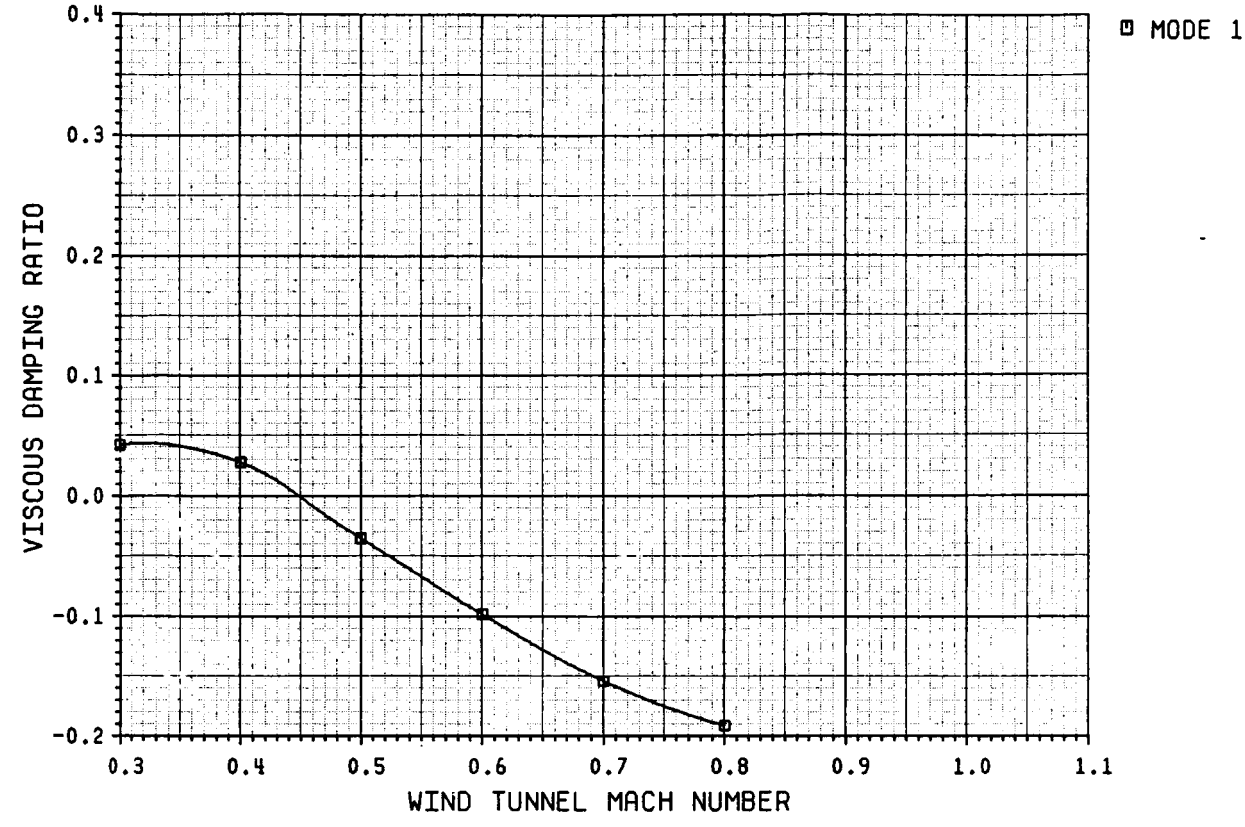

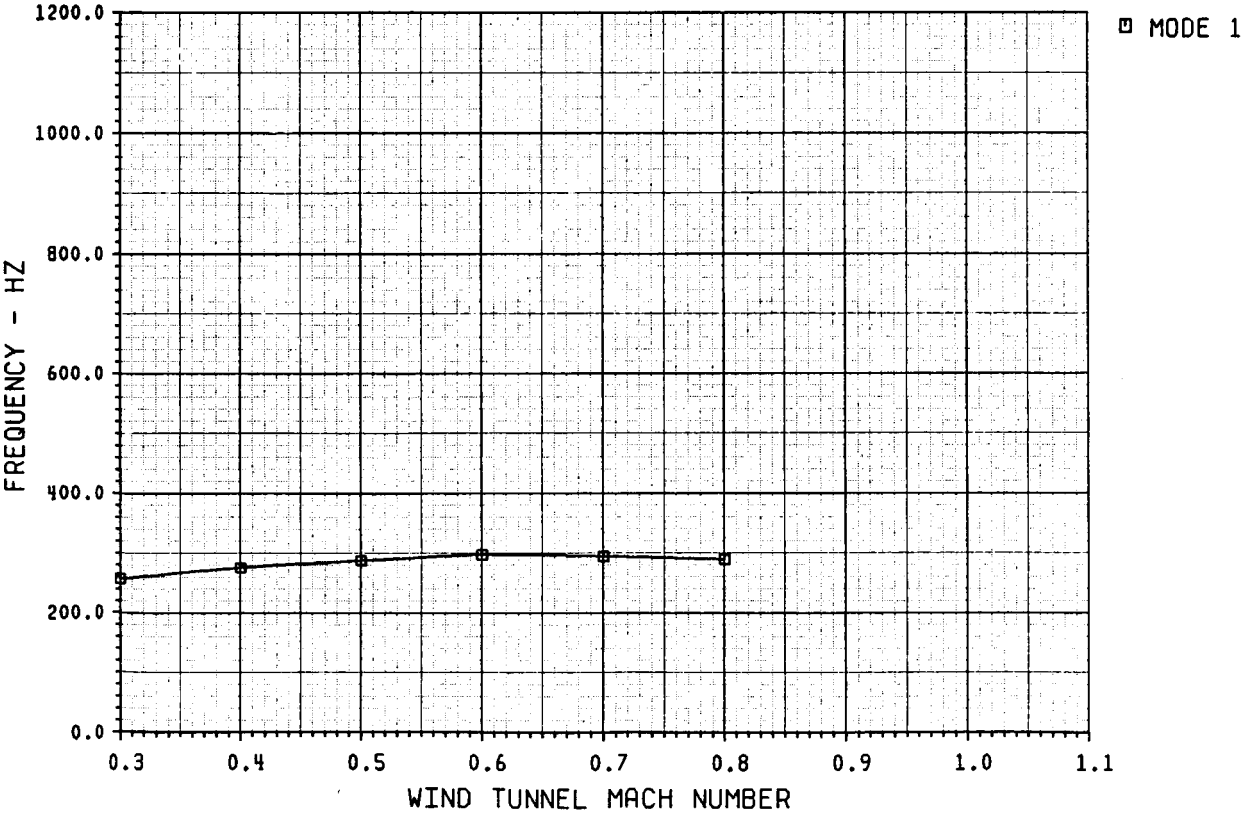

FIGURE 12 SR-3C-X2 STABILITY PREDICTION FOR AN EIGHT-BLADED CONFIGURATION USING CASE 2 MODAL DATA AT 6100 RPM $\beta_{3/4}$ = 61.6°, COSMIC NASTRAN, NO STEADY AIRLOADS

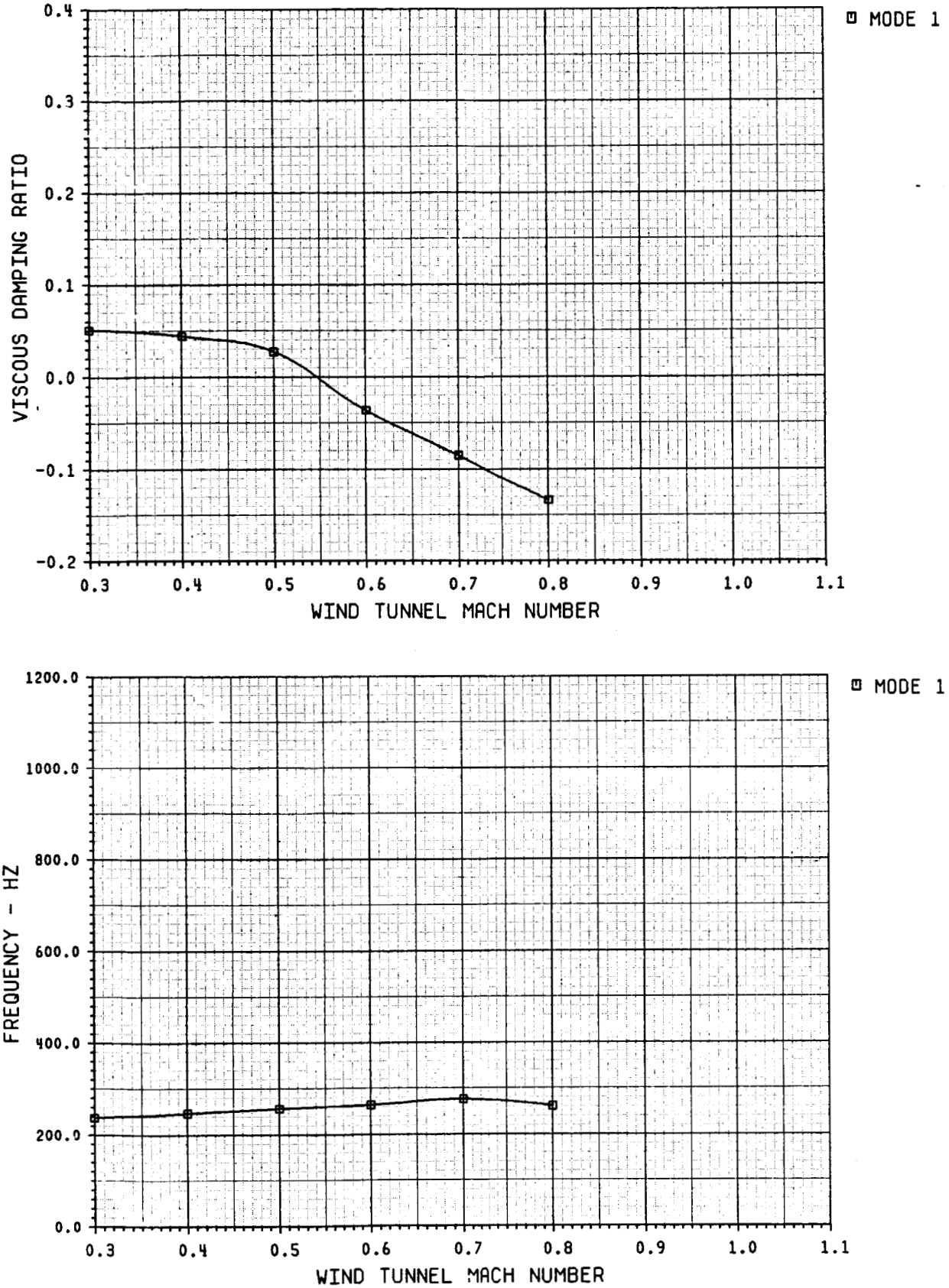

FIGURE 13 SR-3C-X2 STABILITY PREDICTION FOR AN EIGHT-BLADED CONFIGURATION USING CASE 3 MODAL DATA AT 6100 RPM, $\beta_{3/4}$ = 61.6°, MSC NASTRAN, NO STEADY AIRLOADS

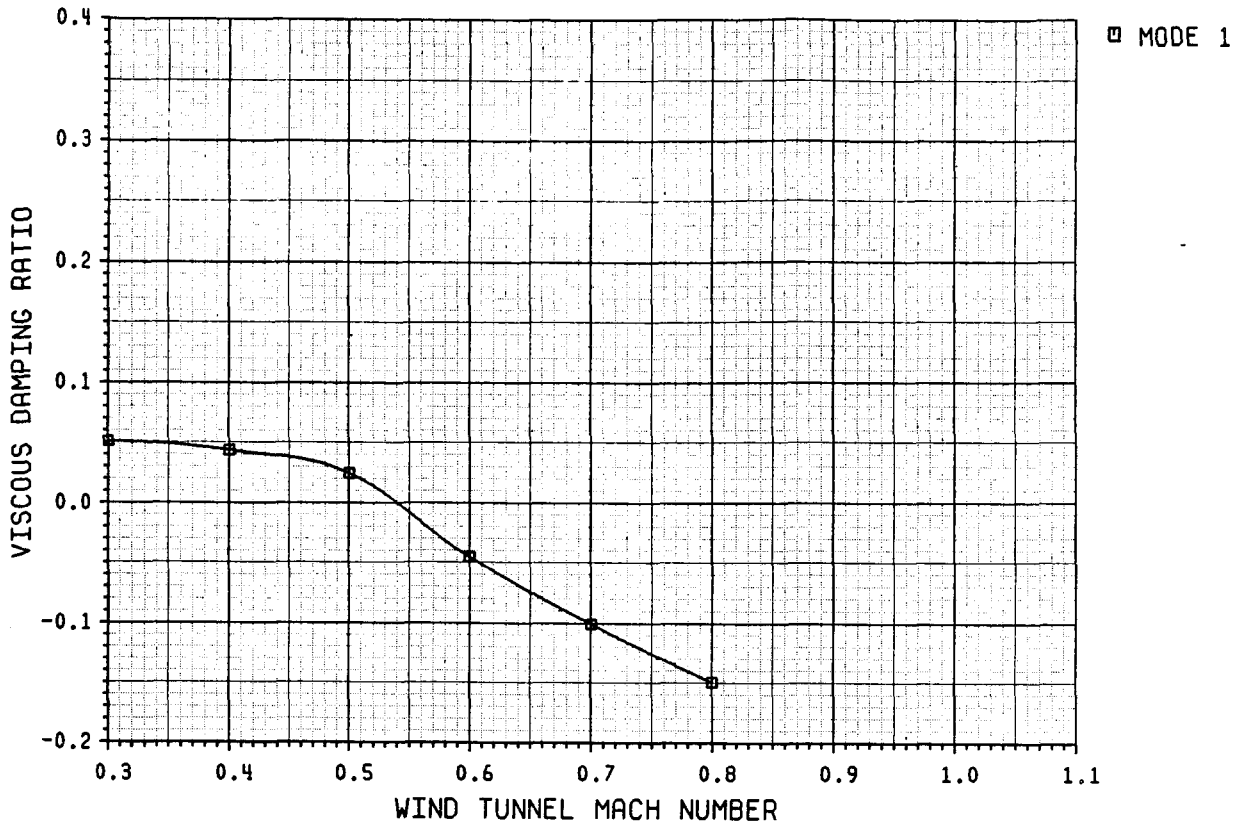

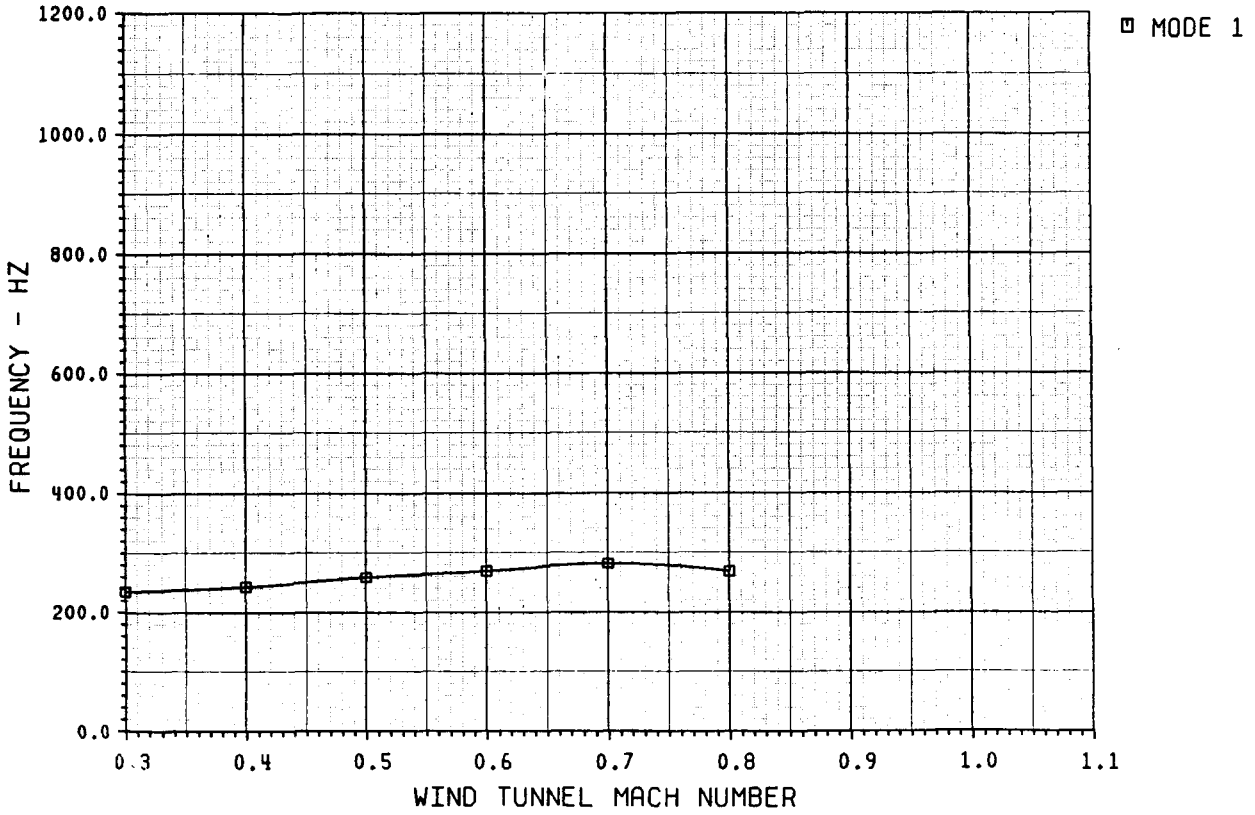

FIGURE 14 SR-3C-X2 STABILITY PREDICTION FOR AN EIGHT-BLADED CONFIGURATION USING CASE 4 MODAL DATA AT 6100 RPM, $\beta_{3/4}$ = 61.6°, MSC NASTRAN, STEADY AIRLOADS

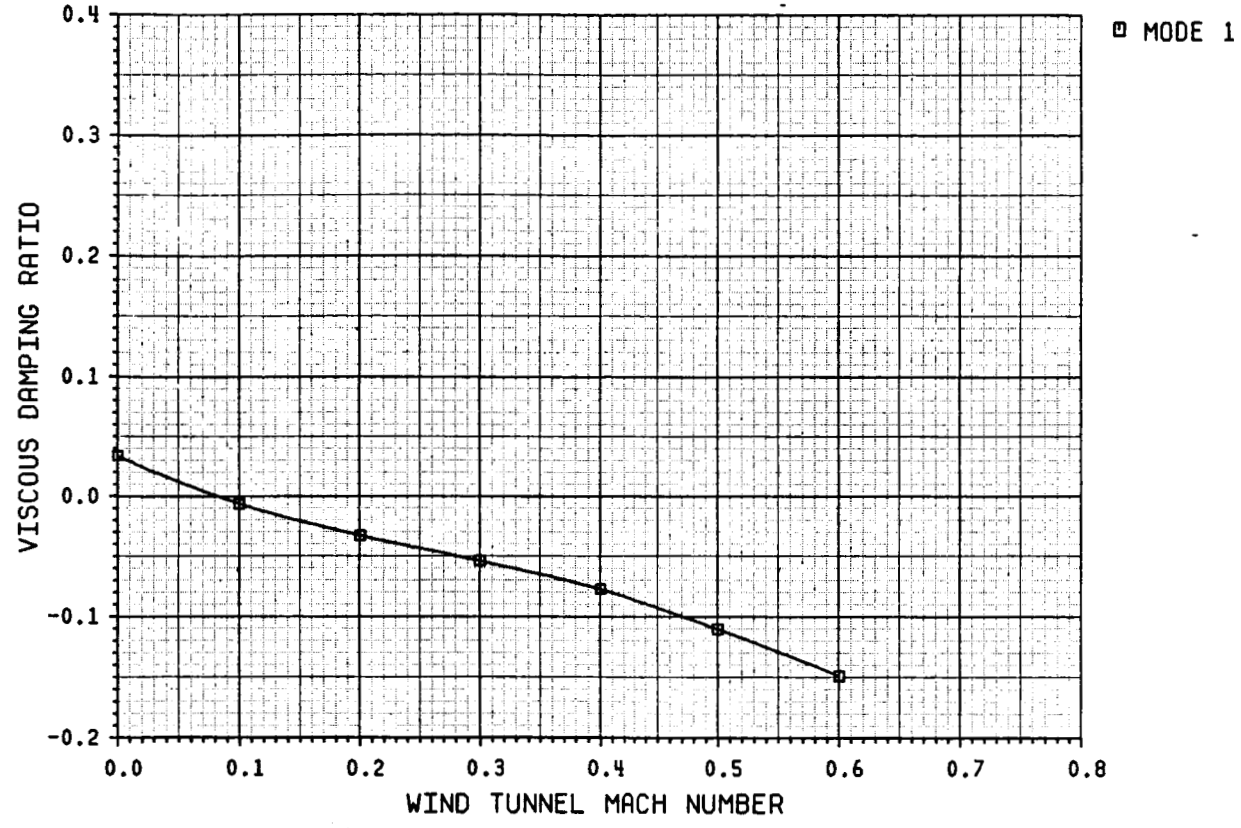

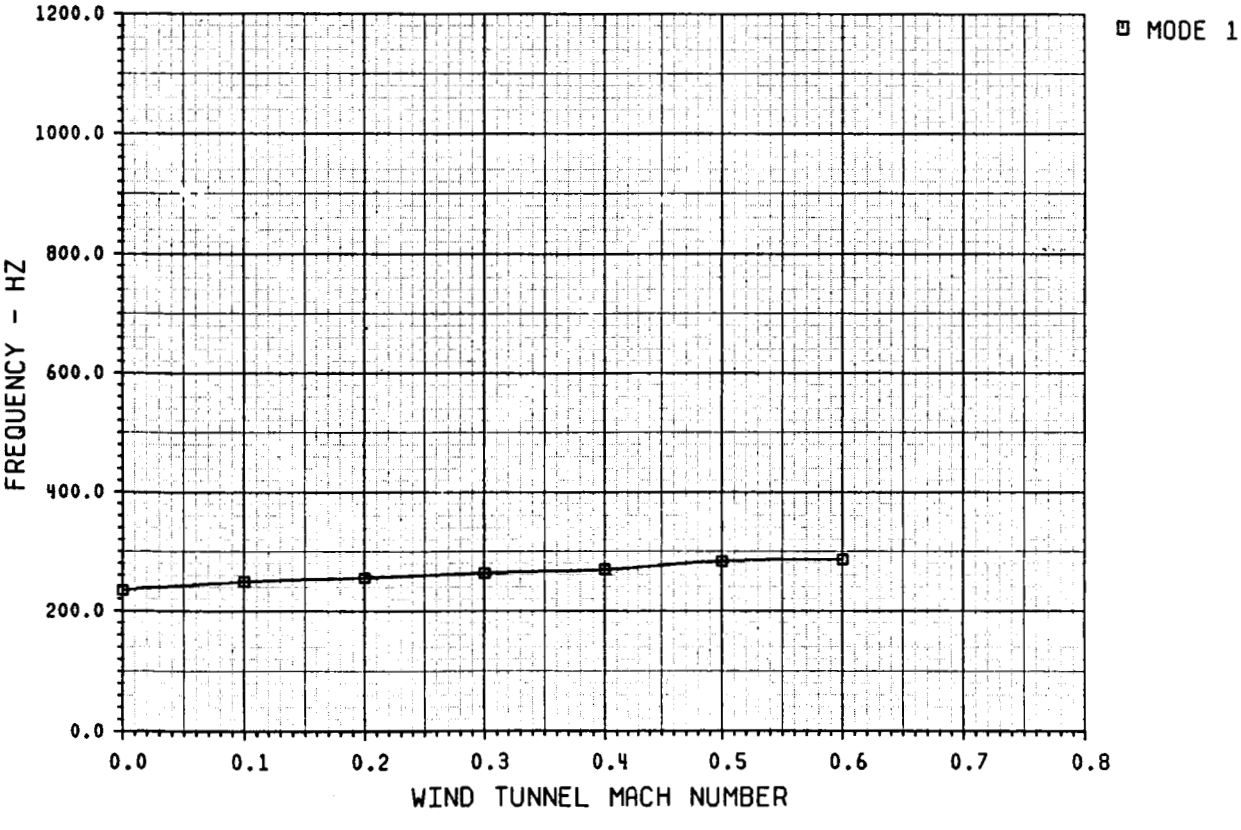

FIGURE 15 SR-3C-X2 STABILITY PREDICTION FOR AN EIGHT-BLADED CONFIGURATION USING CASE 5 MODAL DATA AT 7368 RPM $\beta_{3/4}$ = 61.6°, MSC NASTRAN, STEADY AIRLOADS

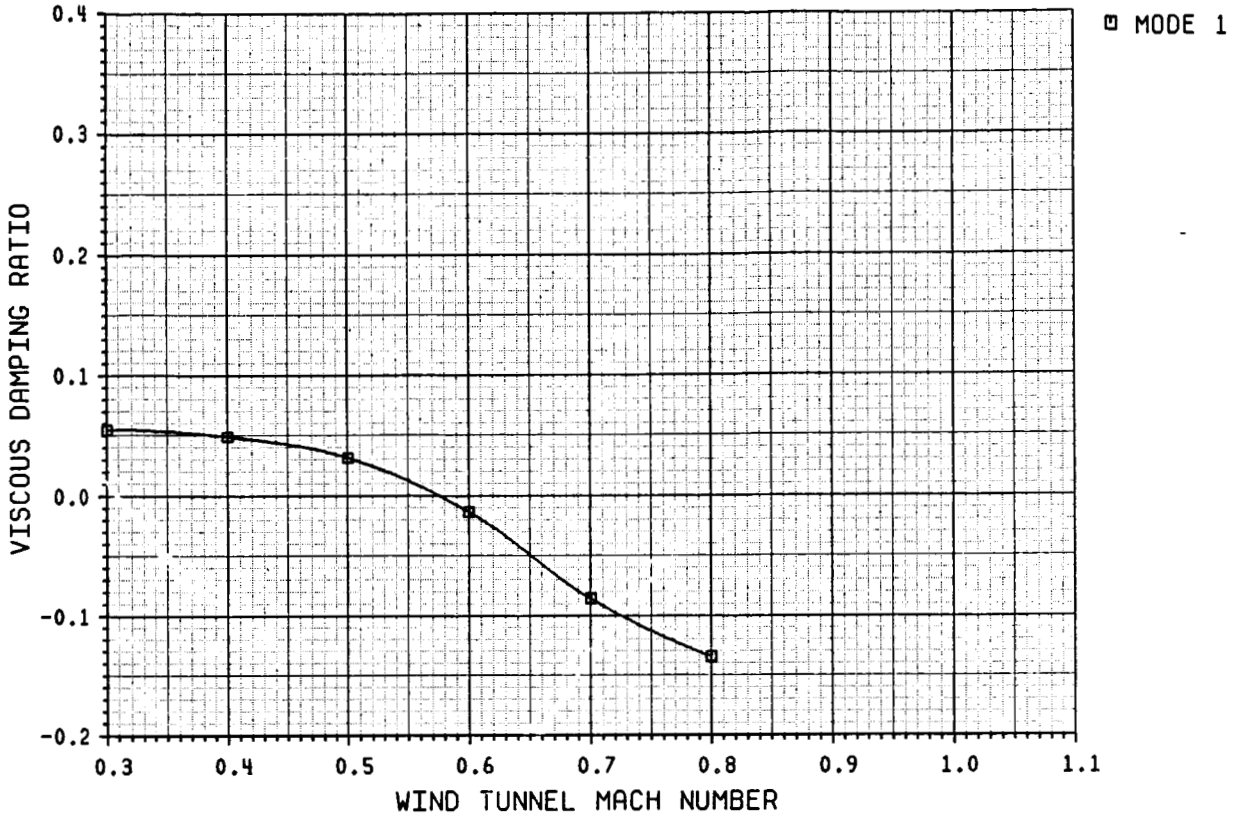

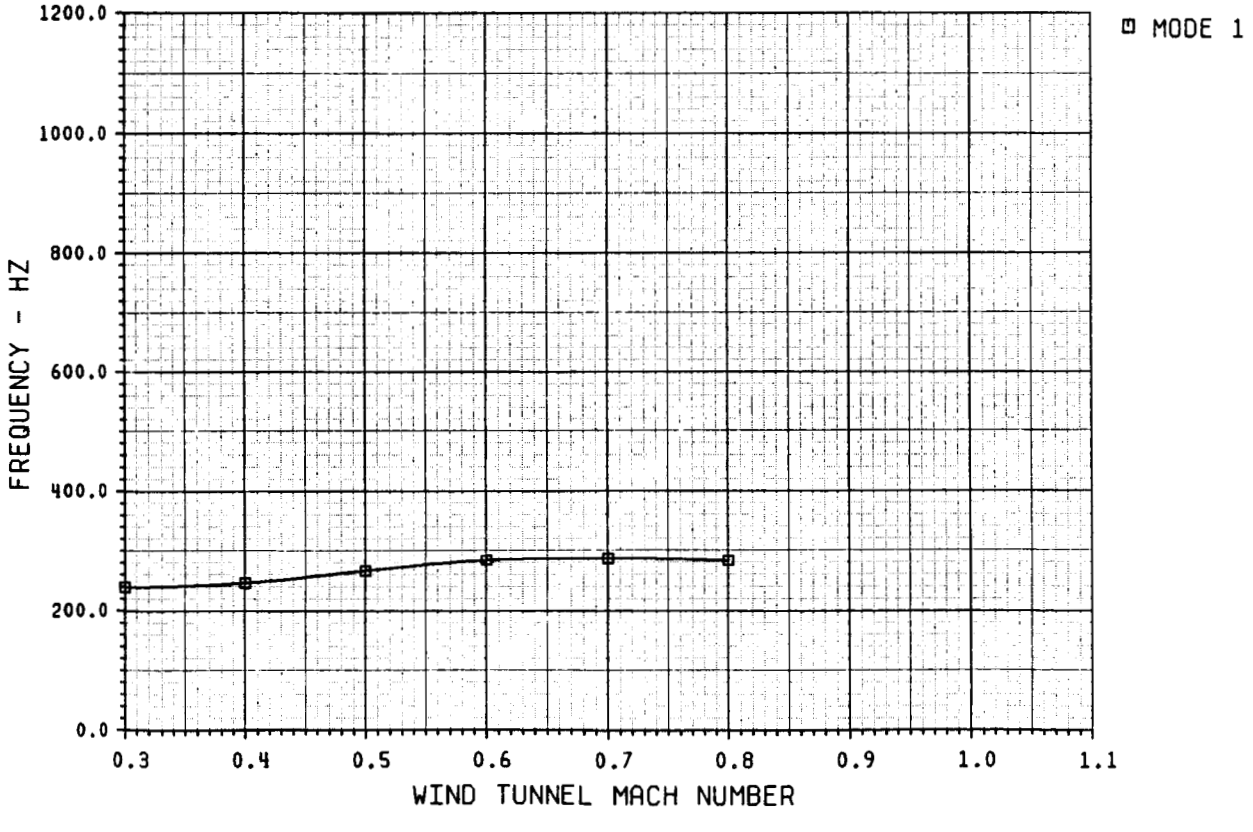

FIGURE 16 SR-3C-X2 STABILITY PREDICTION FOR AN EIGHT-BLADED CONFIGURATION USING CASE 6 MODAL DATA AT 6400 RPM $\beta_{3/4}$ = 56.6°, MSC NASTRAN, STEADY AIRLOADS

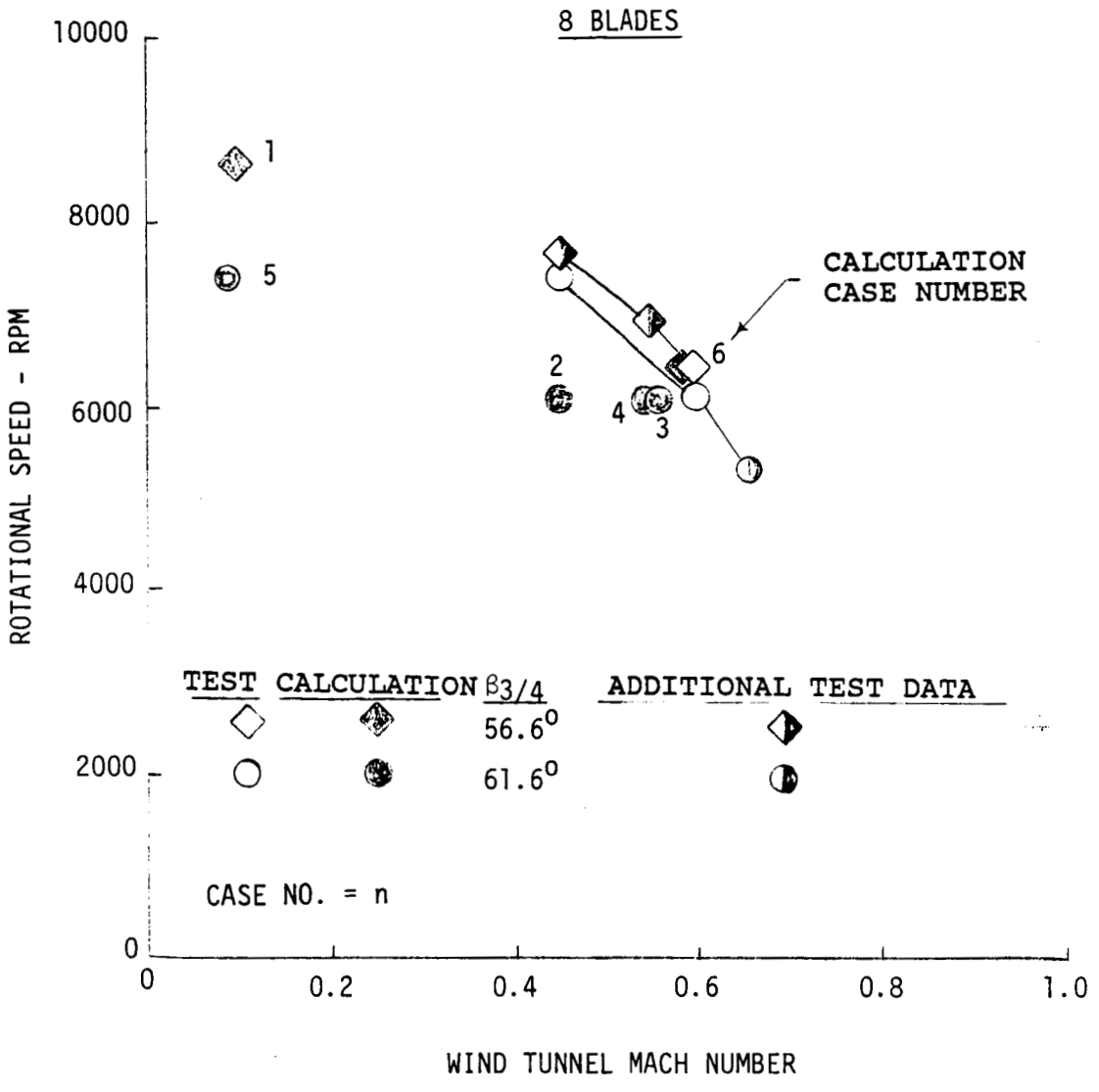

FIGURE 17 A COMPARISON BETWEEN MEASURED AND PREDICTED SR-3C-X2 BLADE STABILITY IN AN EIGHT-BLADED CONFIGURATION

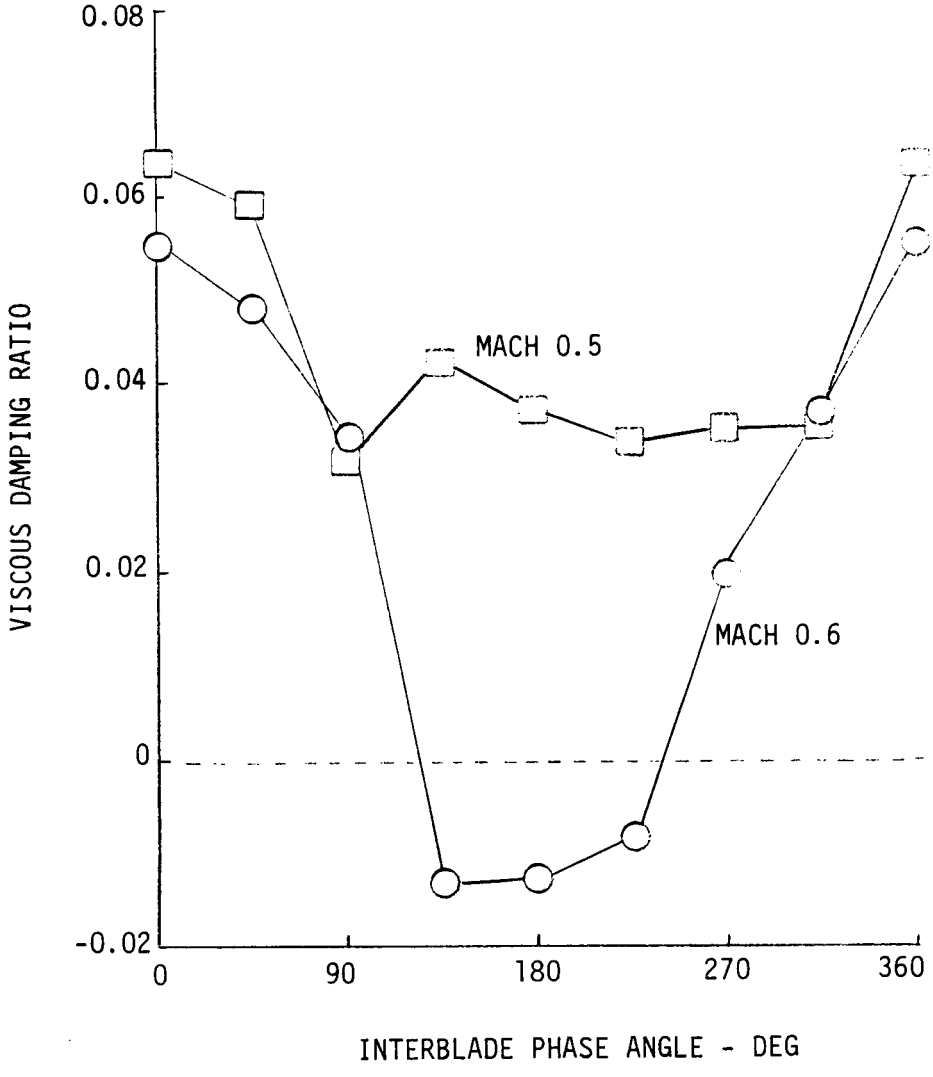

FIGURE 18 PREDICTED INTERBLADE PHASE ANGLE FOR THE SR-3C-X2 USING CASE 6 MODAL DATA AT 6400 RPM 8 BLADES

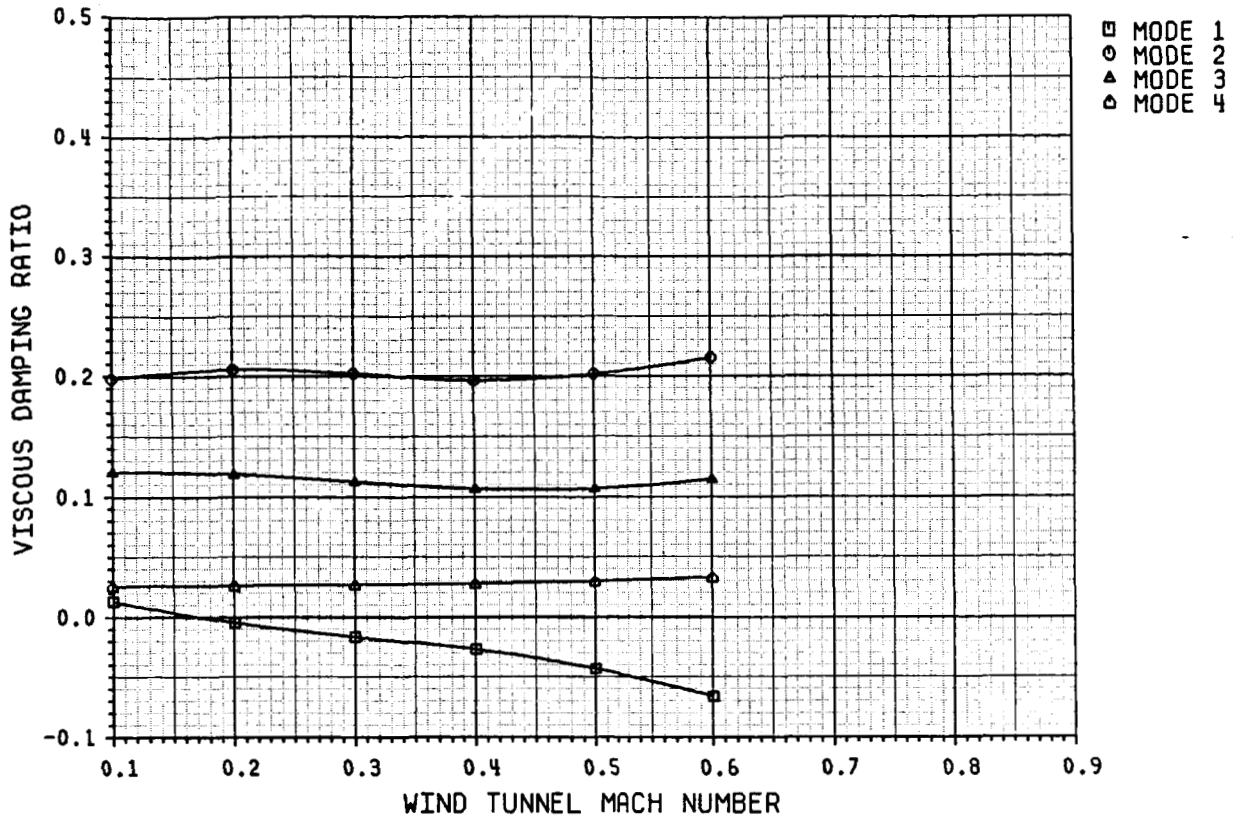

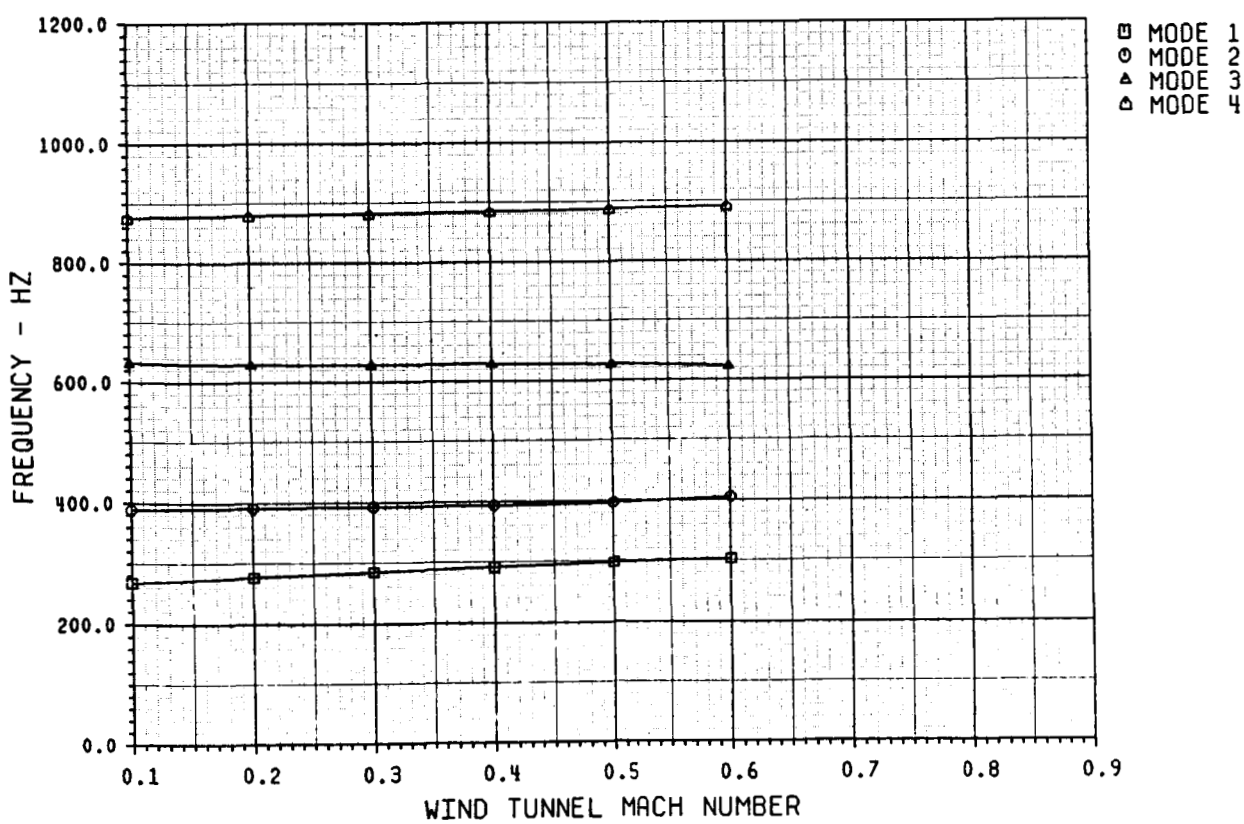

FIGURE 19 SR-3C-X2 STABILITY PREDICTION FOR A FOUR-BLADED CONFIGURATION USING CASE 1 MODAL DATA AT 8636 RPM

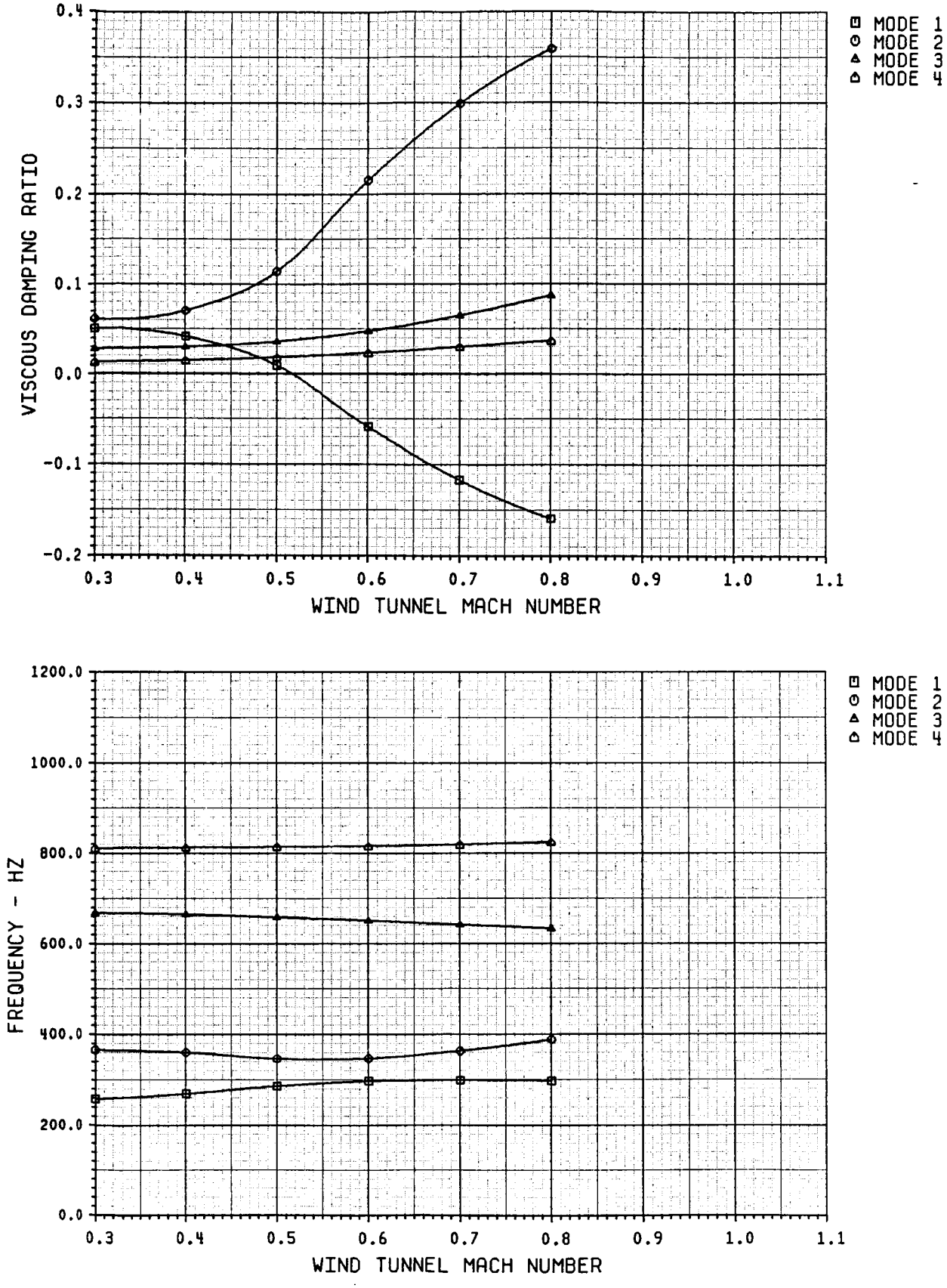

FIGURE 20 SR-3C-X2 STABILITY PREDICTION FOR A FOUR-BLADED CONFIGURATION USING CASE 2 MODAL DATA AT 6100 RPM

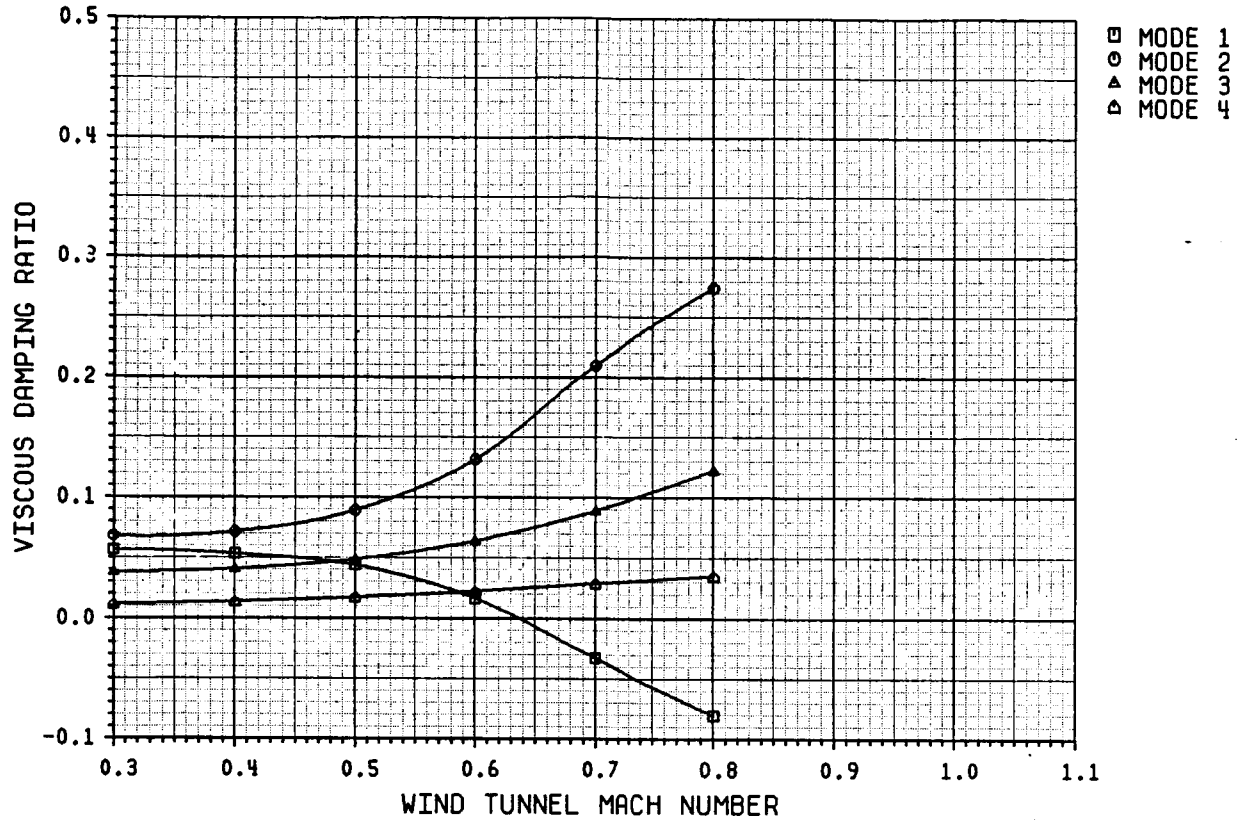

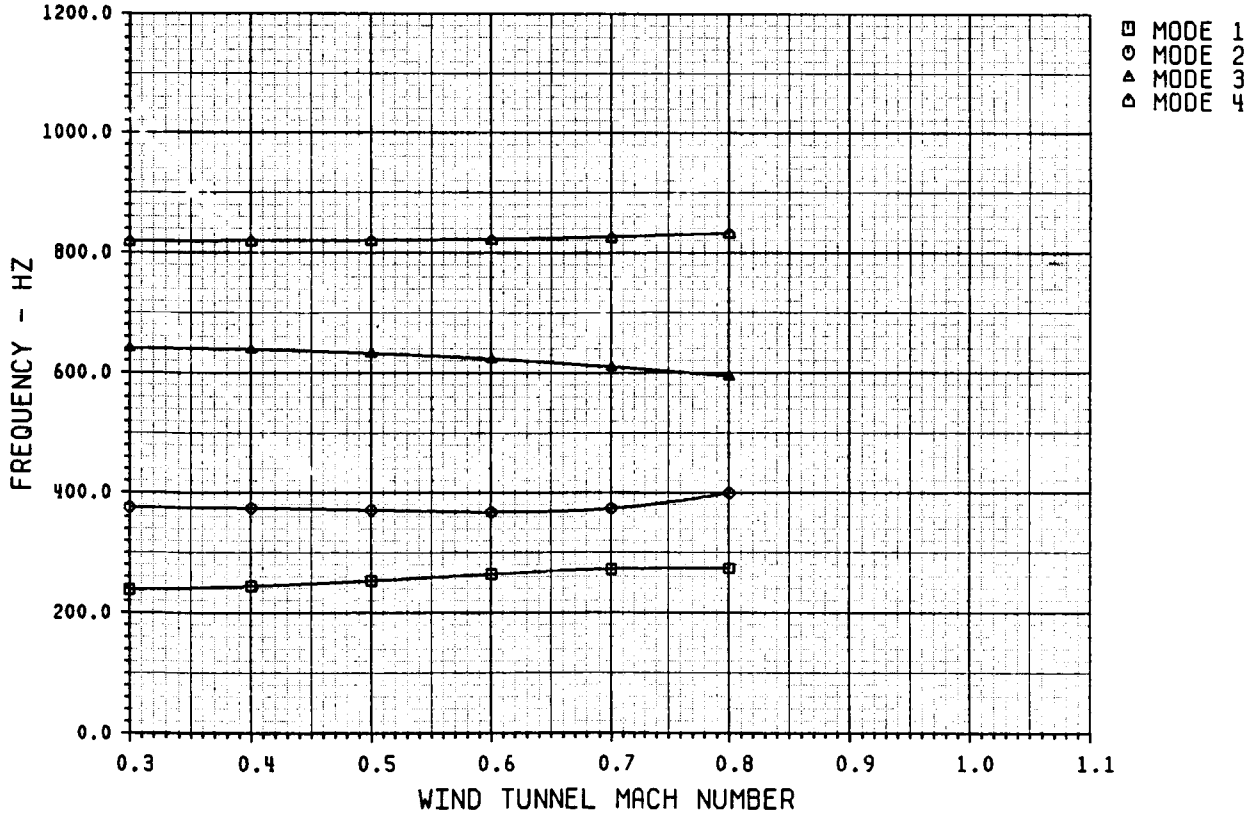

FIGURE 21 SR-3C-X2 STABILITY PREDICTION FOR A FOUR-BLADED CONFIGURATION USING CASE 3 MODAL DATA AT 6100 RPM

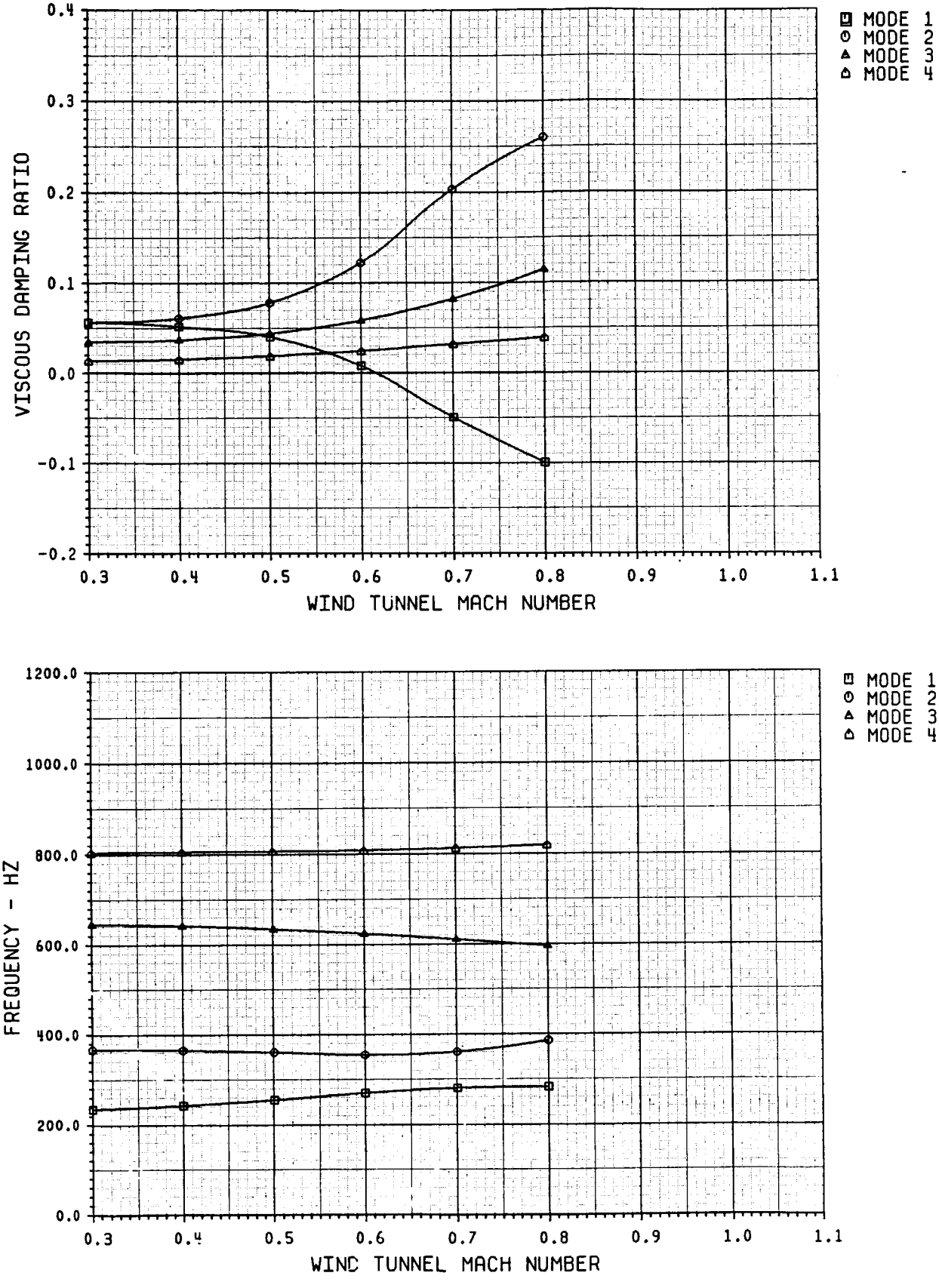

FIGURE 22 SR-3C-X2 STABILITY PREDICTION FOR A FOUR-BLADED CONFIGURATION USING CASE 4 MODAL DATA AT 6100 RPM

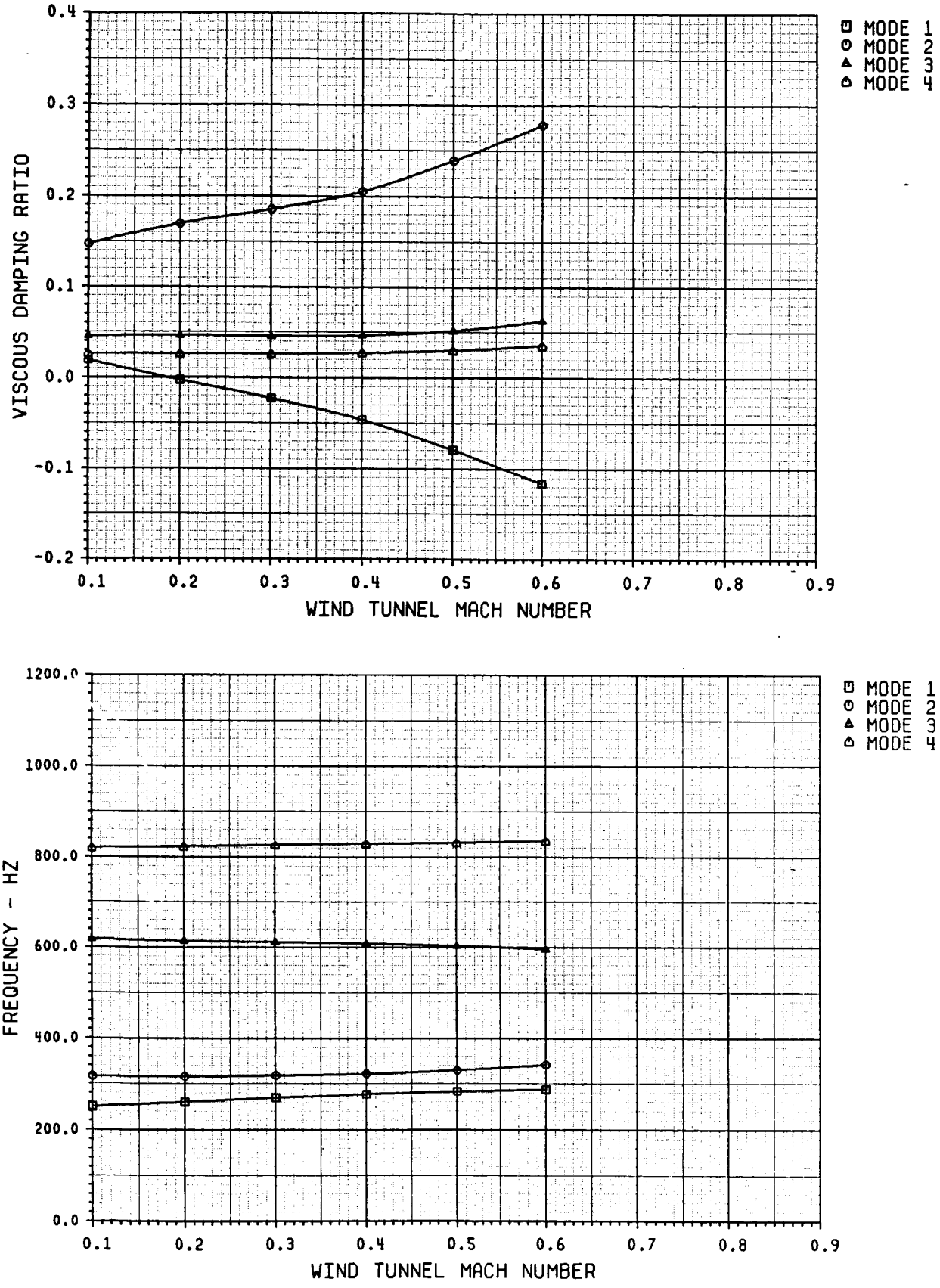

FIGURE 23 SR-3C-X2 STABILITY PREDICTION FOR A FOUR-BLADED CONFIGURATION USING CASE 5 MODAL DATA AT 7368 RPM

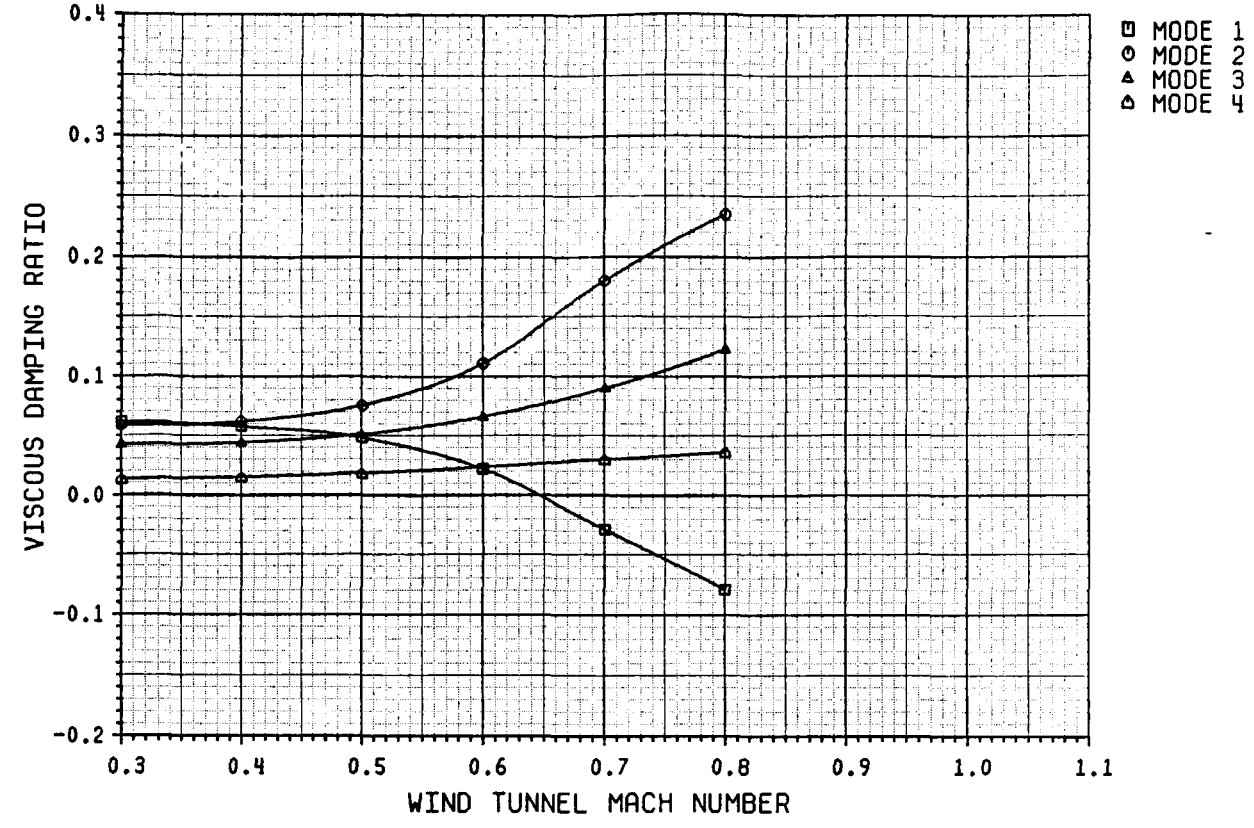

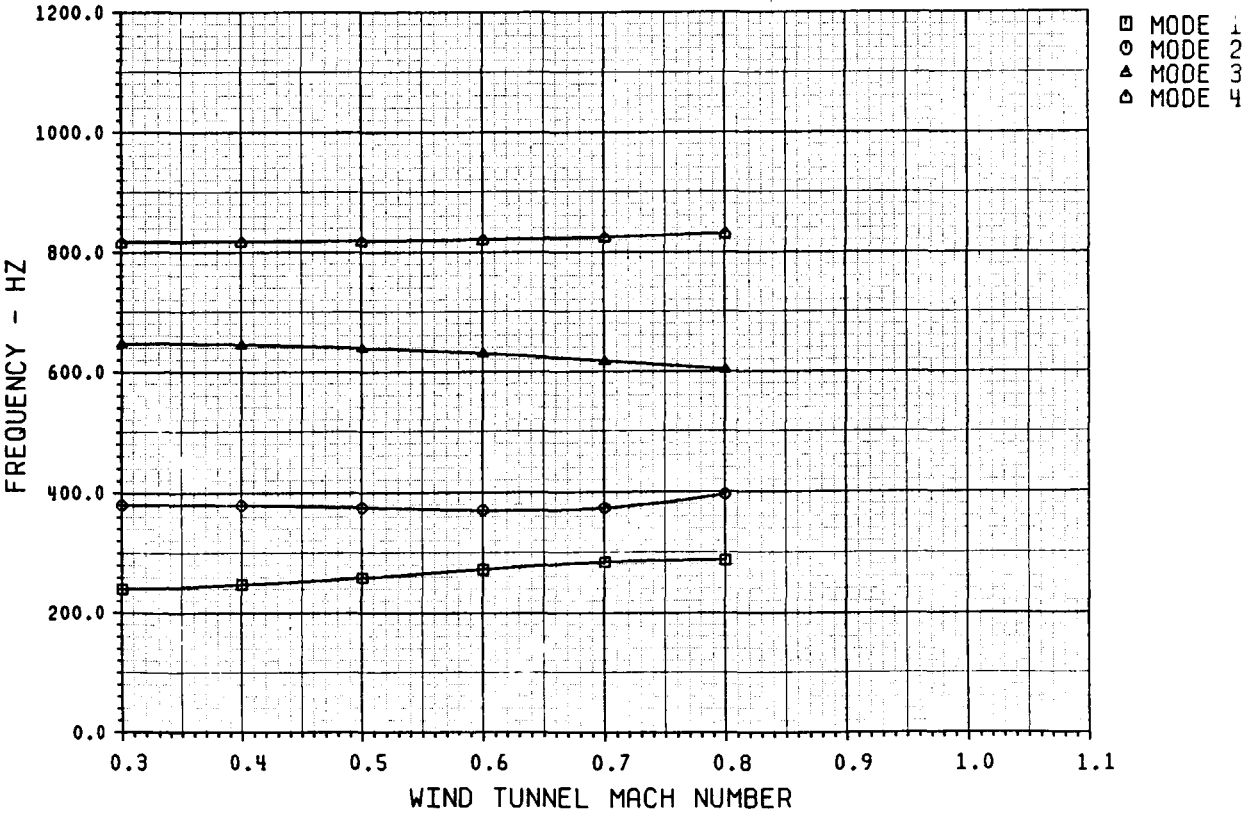

FIGURE 24 SR-3C-X2 STABILITY PREDICTION FOR A FOUR-BLADED CONFIGURATION USING CASE 6 MODAL DATA AT 6400 RPM

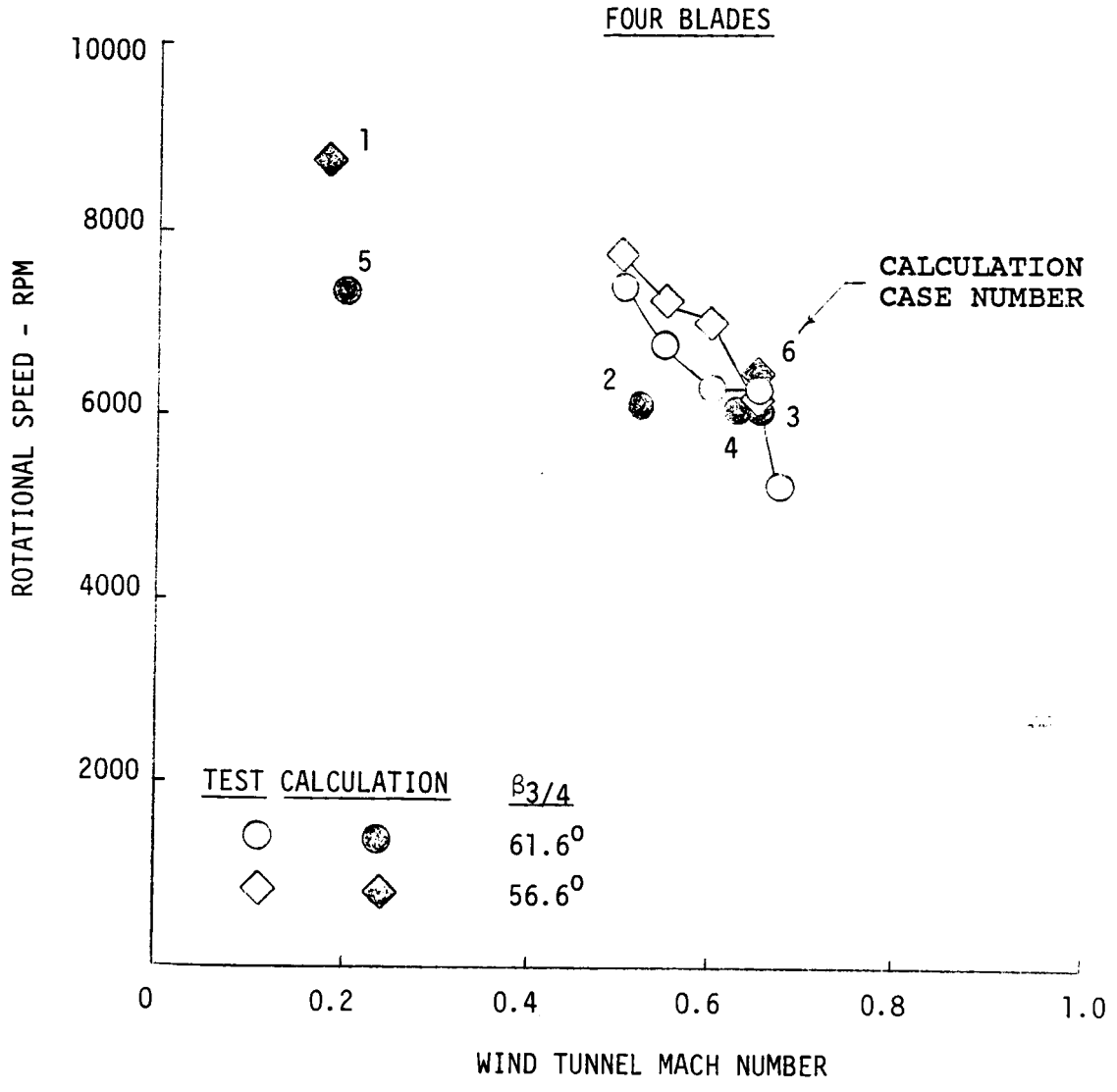

FIGURE 25 A COMPARISON BETWEEN MEASURED AND PREDICTED SR-3C-X2 BLADE STABILITY IN A FOUR-BLADED CONFIGURATION